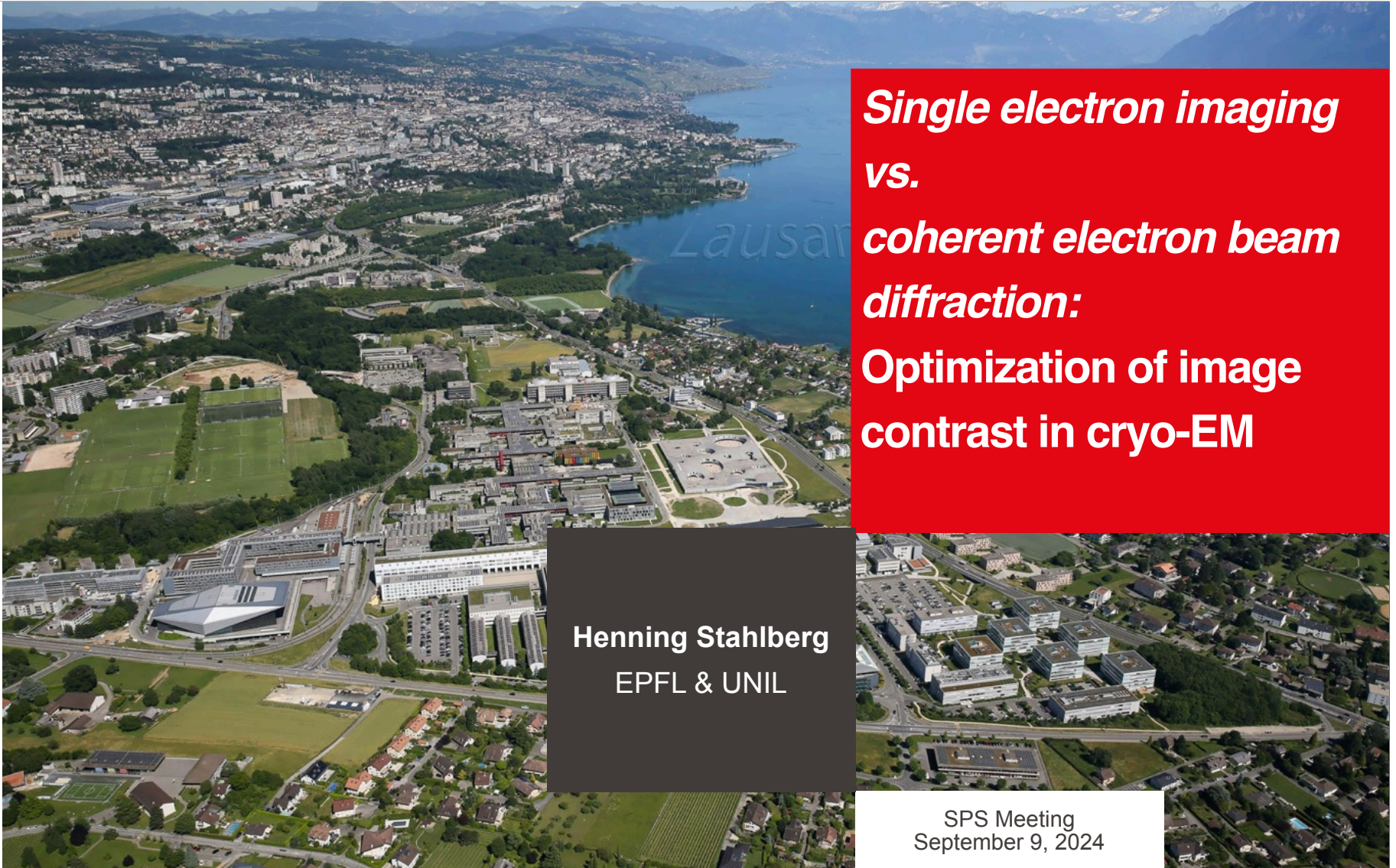


EPFL

Unil
UNIL | Université de Lausanne

Laboratory of Biological
Electron Microscopy

■ LBEM



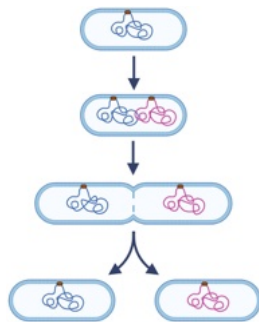
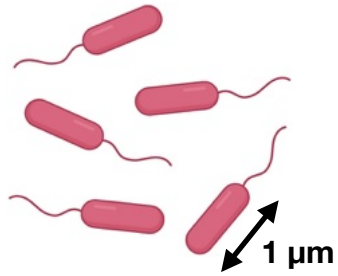
***Single electron imaging
vs.
coherent electron beam
diffraction:
Optimization of image
contrast in cryo-EM***

Henning Stahlberg
EPFL & UNIL

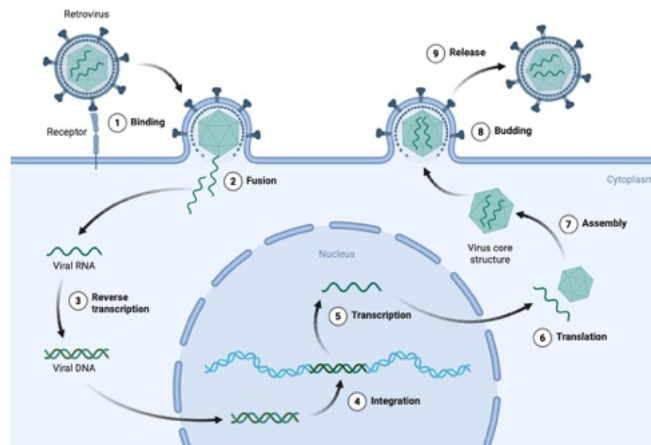
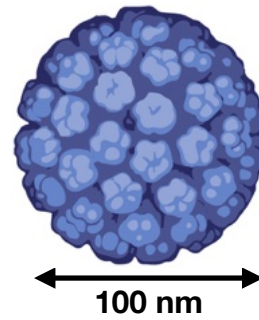
SPS Meeting
September 9, 2024

Bacteria, Viruses, and Prions

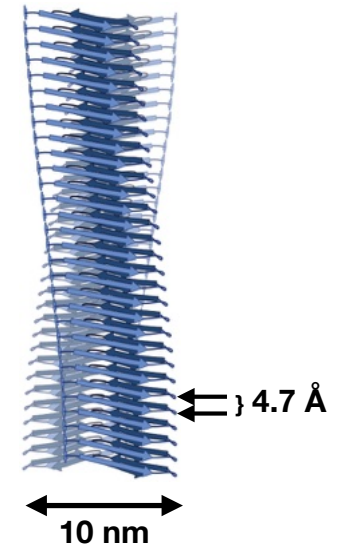
Bacteria



Viruses

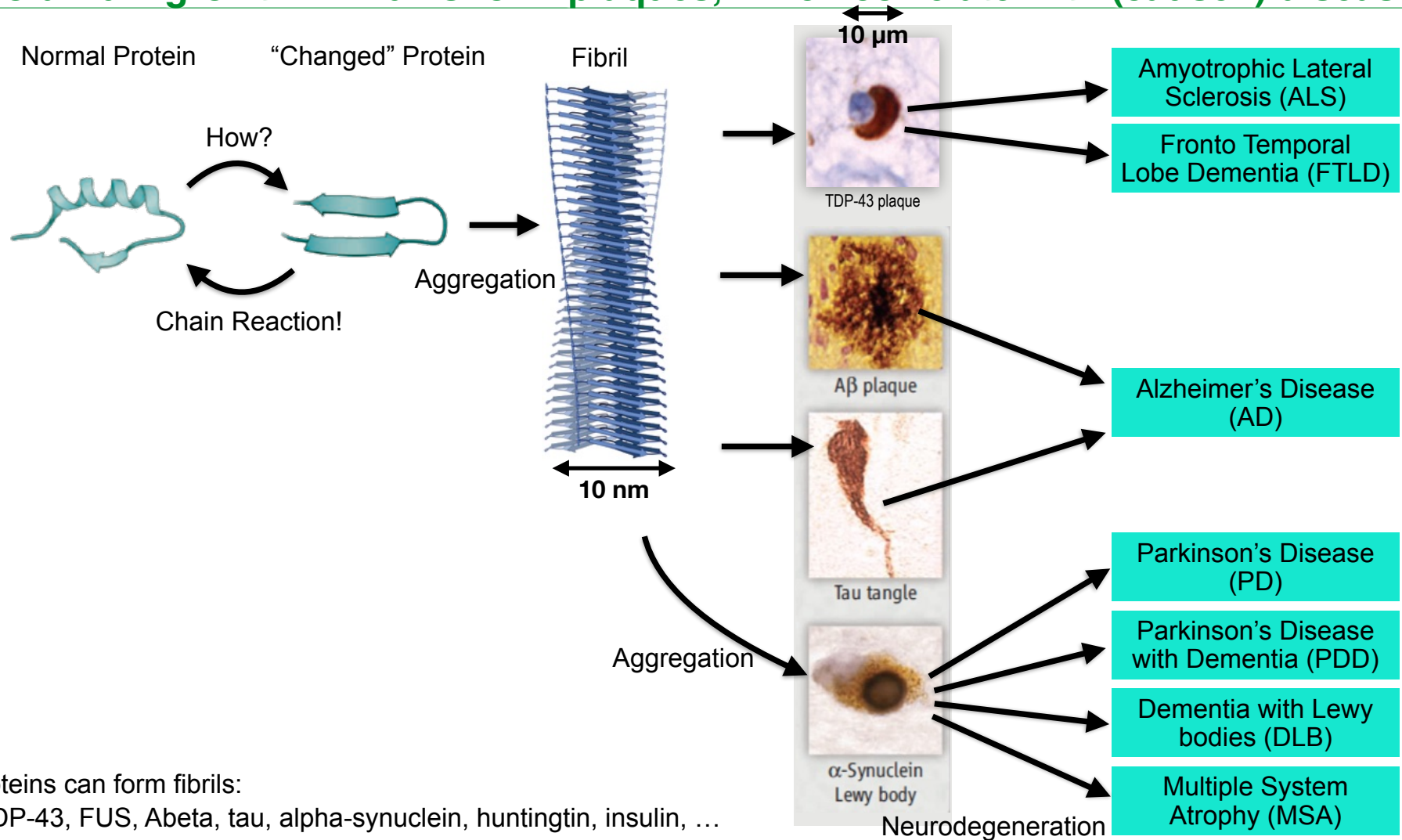


Fibrils



Created with BioRender.com

Prionoid fibril growth: Fibrils form plaques, which correlate with (cause?) disease



Many proteins can form fibrils:
PrP^{Sc}, TDP-43, FUS, Abeta, tau, alpha-synuclein, huntingtin, insulin, ...

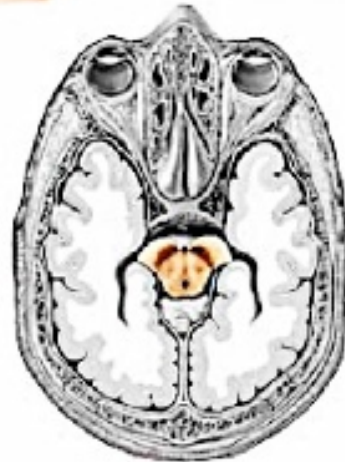
Parkinson's Disease: Lewy bodies contain the protein alpha-synuclein



<https://www.youtube.com/watch?v=2Z4Vl3HlnA>, 19.4.2017



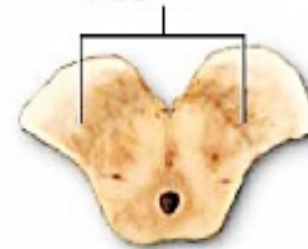
Cut section of the midbrain where a portion of the substantia nigra is visible



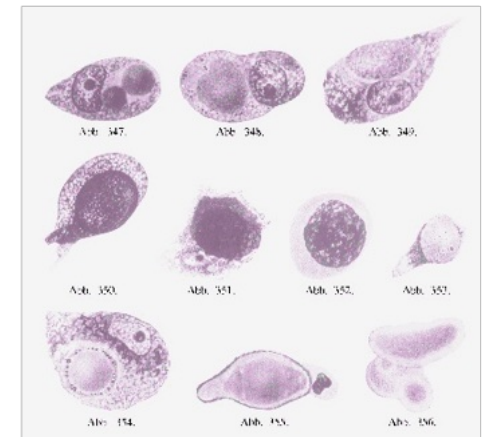
Substantia nigra



Diminished substantia nigra as seen in Parkinson's disease



Friedrich Heinrich Lewy
(1885 – 1950)

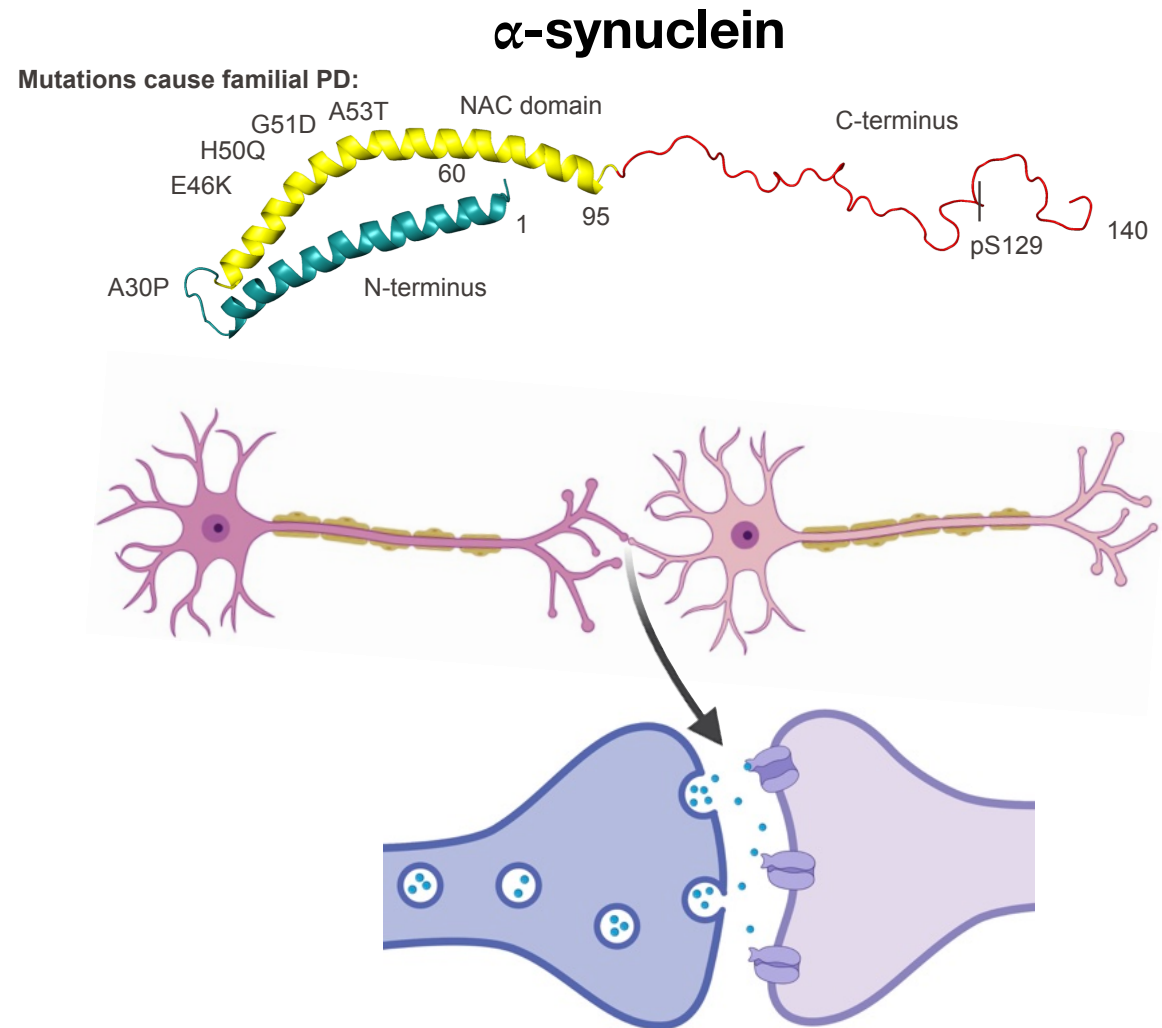


A figure from Lewy's *Tonus und Bewegung* (1923), showing images of Lewy bodies

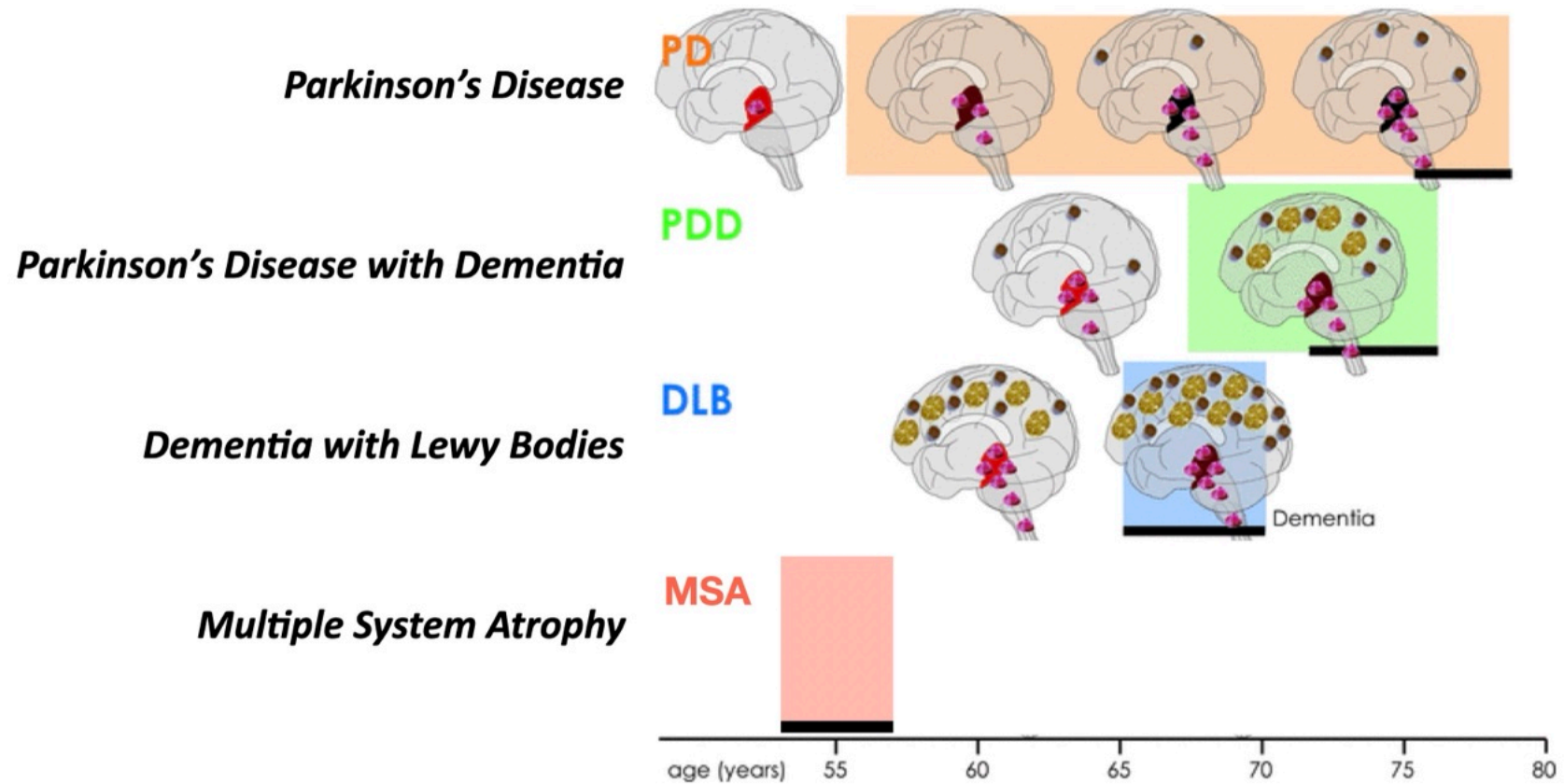
“Lewy” bodies in the brain.
These are full of alpha-synuclein.

alpha-synuclein is a small protein, found at high concentration in Lewy bodies

- 14 kDa weight
- 140 amino acids
- Natively unfolded
- Membrane interacting (Nanodisks? Pores?)
- α -helical in contact with membranes
- β -sheet in fibrils
- Mutations can cause familial PD (A30P, E46K, H50Q, G51D, A53T)



Synucleinopathies: Different “strains” of α -synuclein fibrils may cause different diseases



Other diseases related to α Syn fibrils

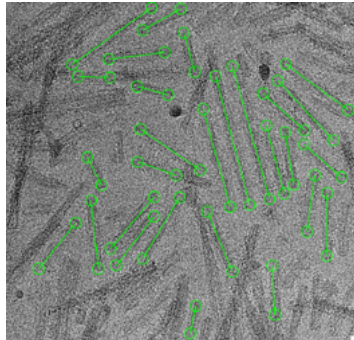
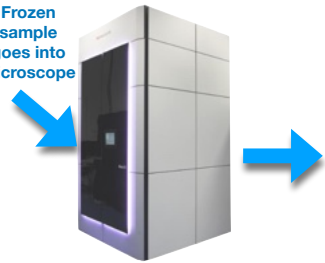
- Lewy Body variant of Alzheimer's Disease (AD)
- Neurodegeneration with Brain Iron Accumulation (NBIA) Type I
- Pure Autonomic Failure (PAF) Disease

Modified from: Halliday & McCann, *Annals of the New York Academy of Sciences* 1184(1), 188-195 (2010)

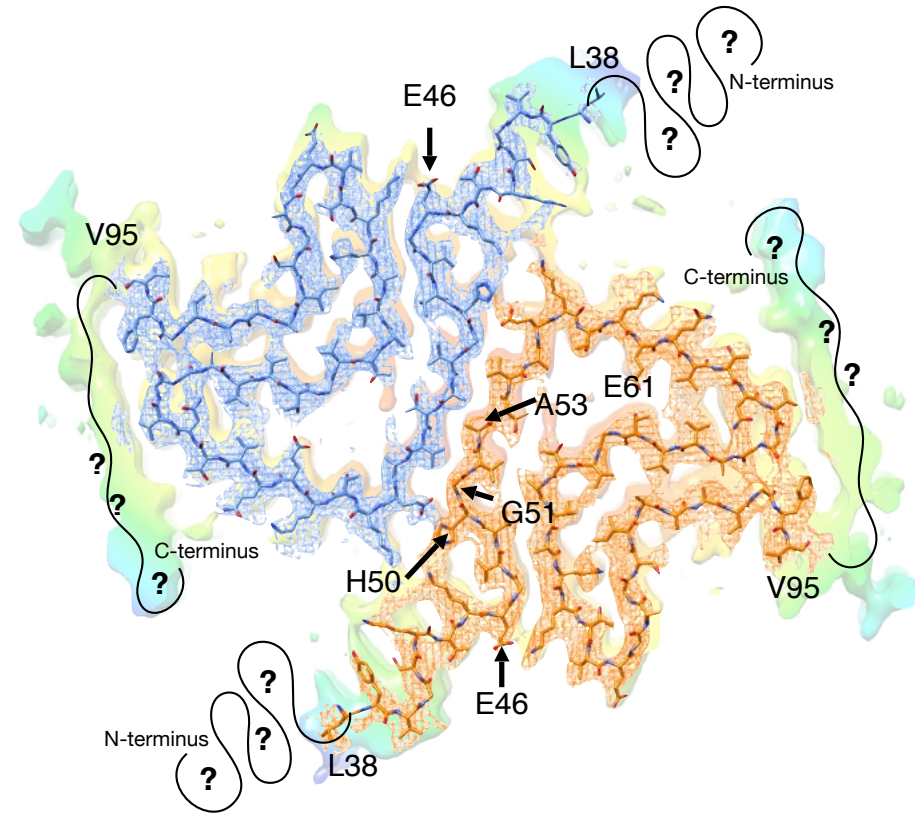
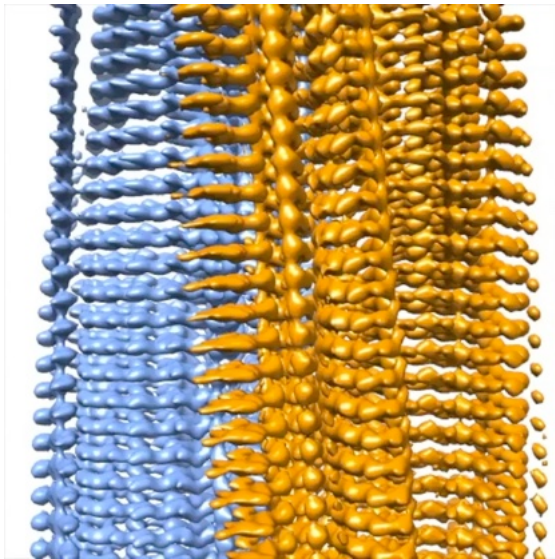
In vitro generated aSyn fibrils

Ricardo Guerrero, with Markus Britschgi (Roche) and Roland Riek (ETHZ)

Frozen sample goes into microscope



Cryo-EM image of fibrils
(10'000 fibril images are needed)

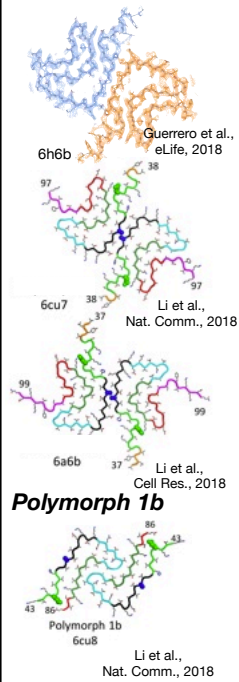


Guerrero-Ferreira et al., eLife (2018, 2019)

Alpha-Synuclein Fibril Polymorphism

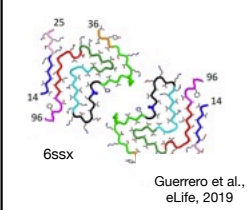
In vitro, wt

Polymorph 1a

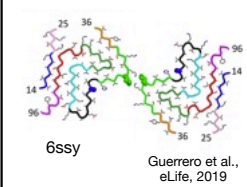


In vitro, wt

Polymorph 2a

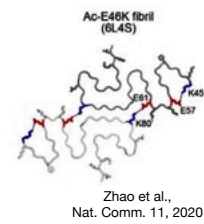


Polymorph 2b



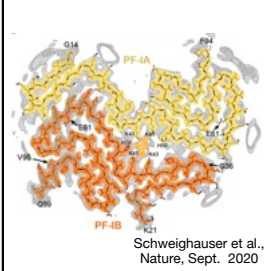
In vitro, Ac-E46K

Polymorph 3a

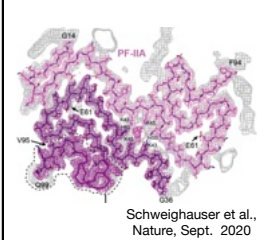


MSA brain purified

Polymorph 4a



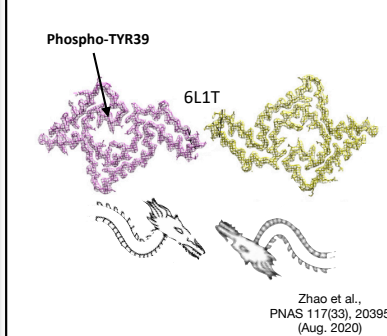
Polymorph 4b



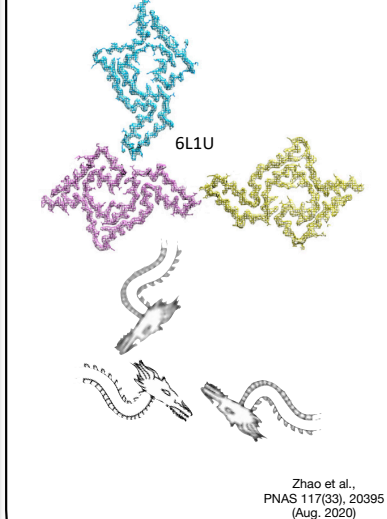
(sarkosyl, ultrasound)

In vitro, pTYR39

Polymorph 5a

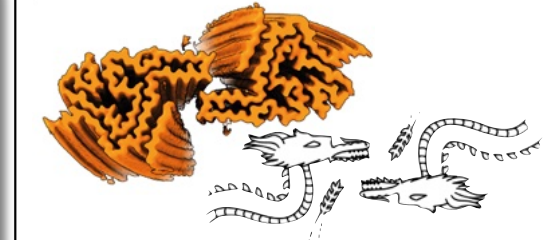


Polymorph 5b



PD & MSA brain seeded (PMCA)

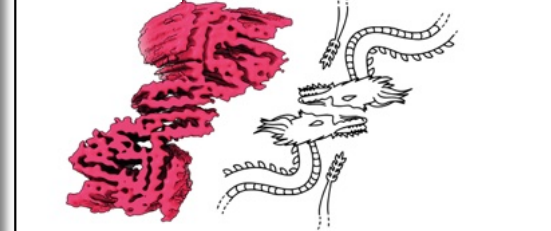
Polymorph 6a



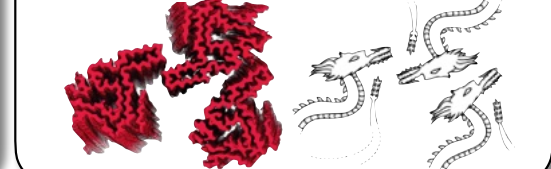
Polymorph 6b



Polymorph 6c



Polymorph 6D



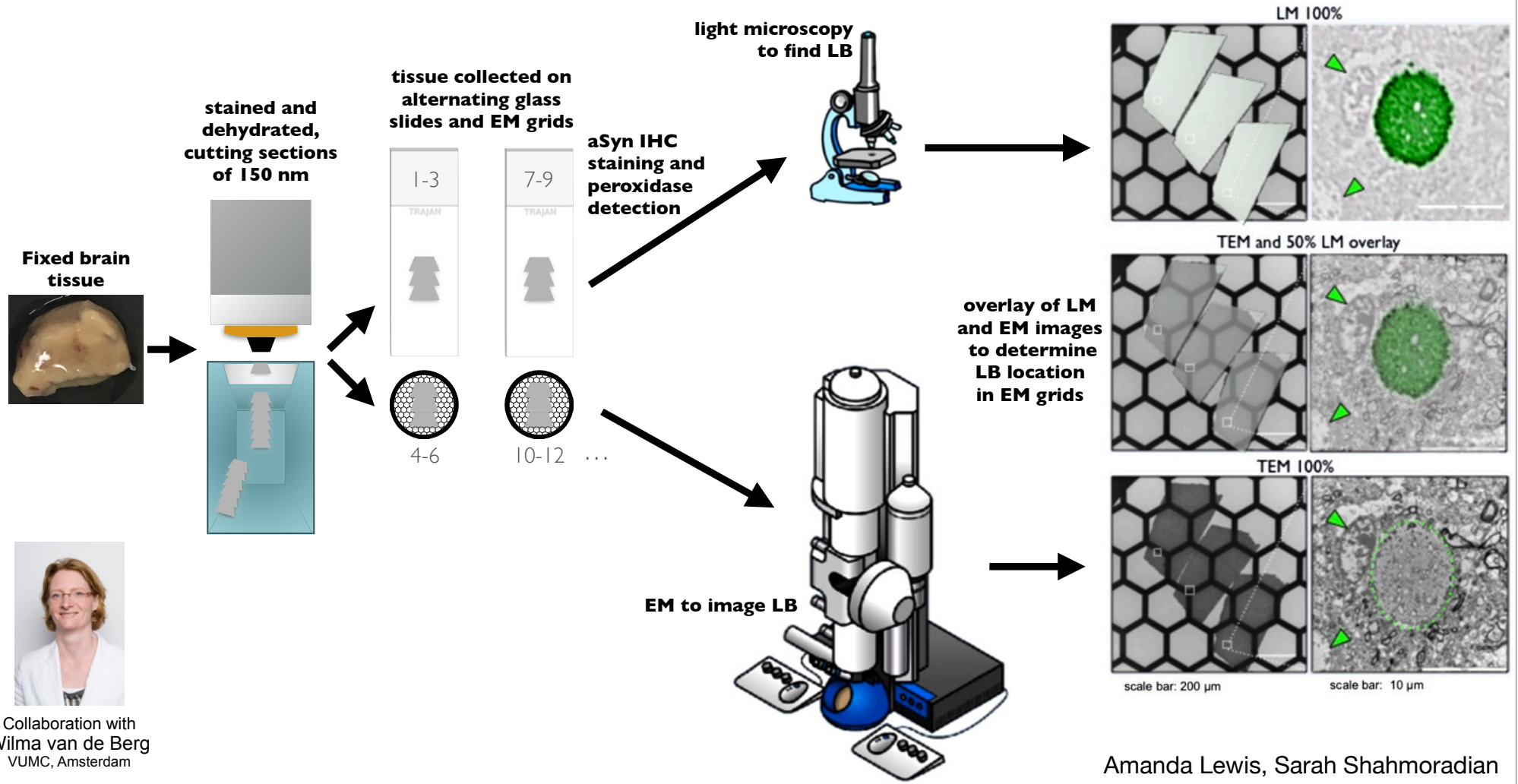
Domenic Burger (EDNE)

Cryo-EM of the human brain suffering from neurodegeneration

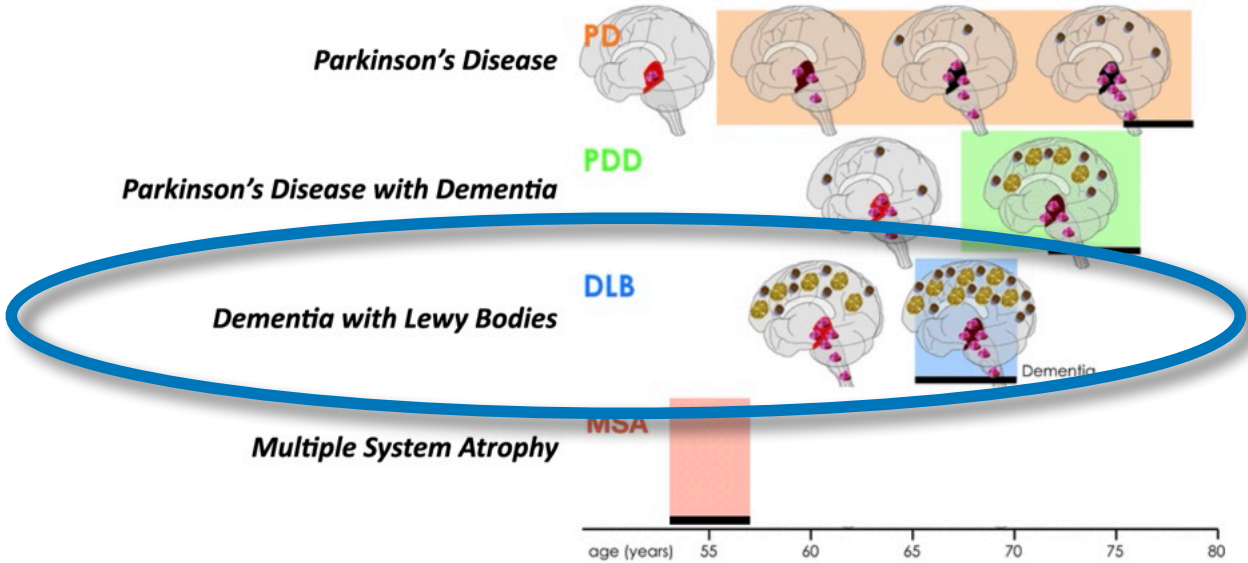


*What is the
mechanism of neurodegeneration
in the human brain ?*

CLEM - Correlative Light and Electron Microscopy

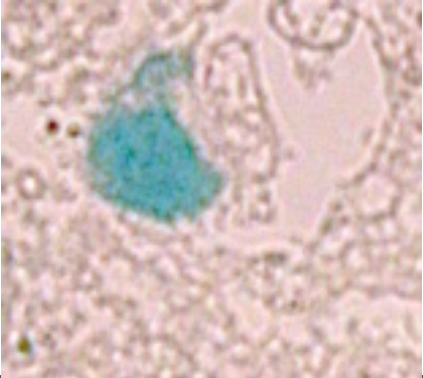


Dementia with Lewy bodies (DLB)



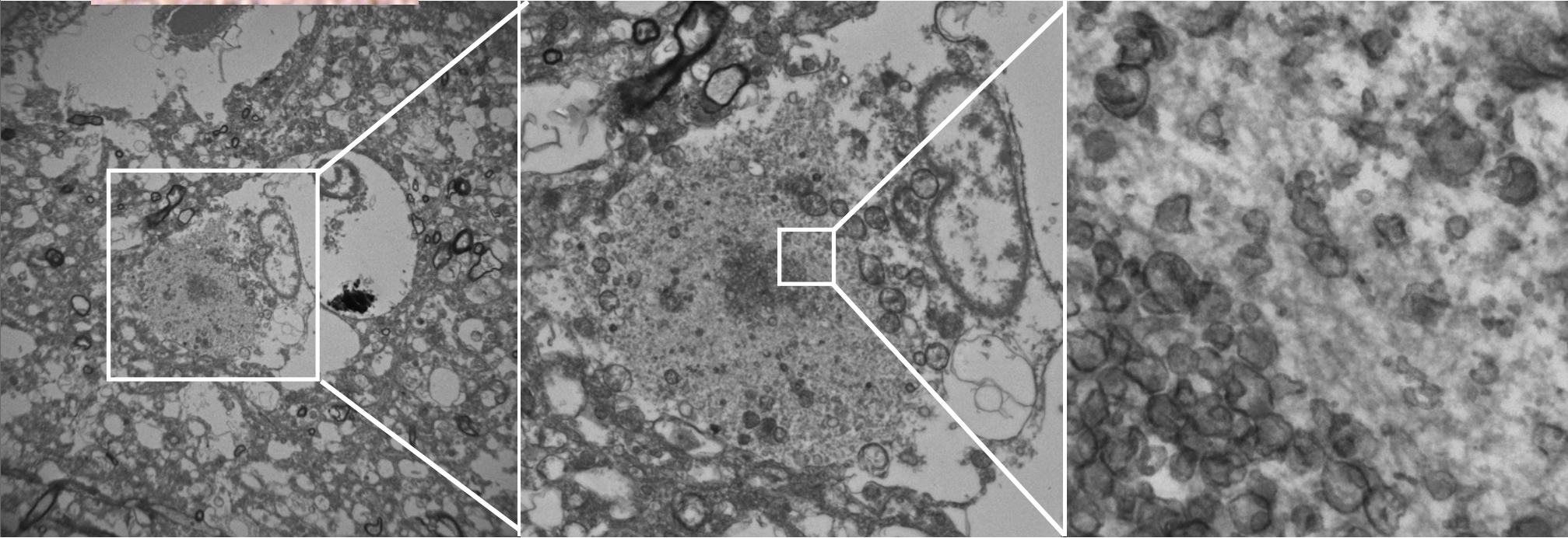
DLB: CLEM image of a Cingulate Gyrus of a DLB patient

Notash Shafiei, LBEM

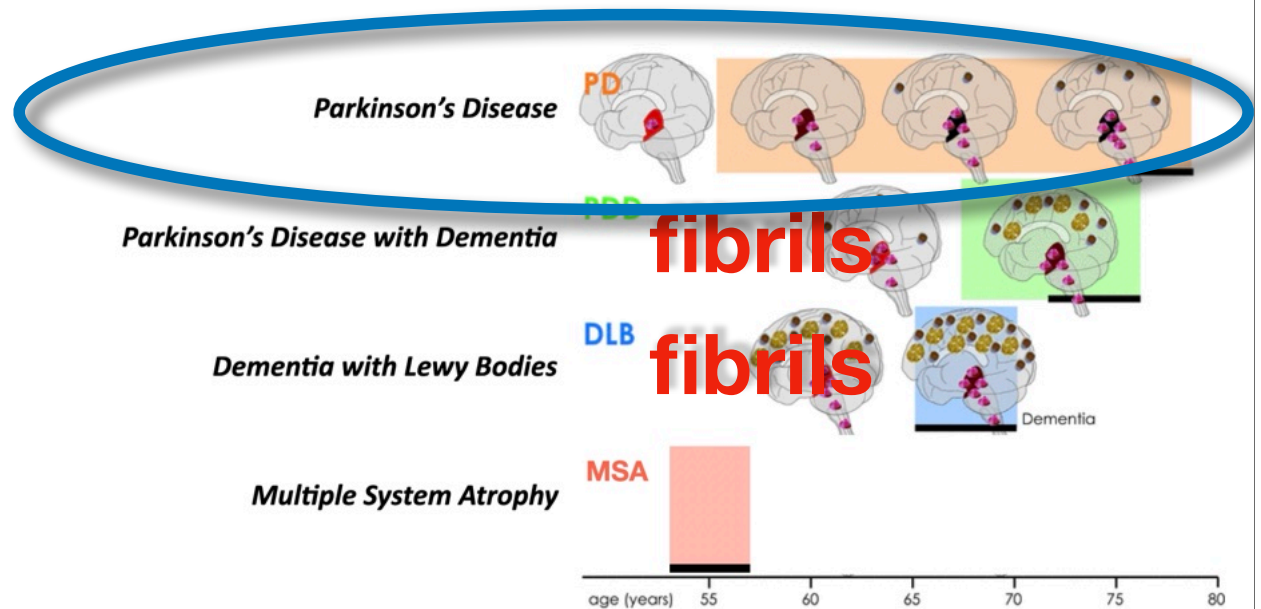


Light Microscopy

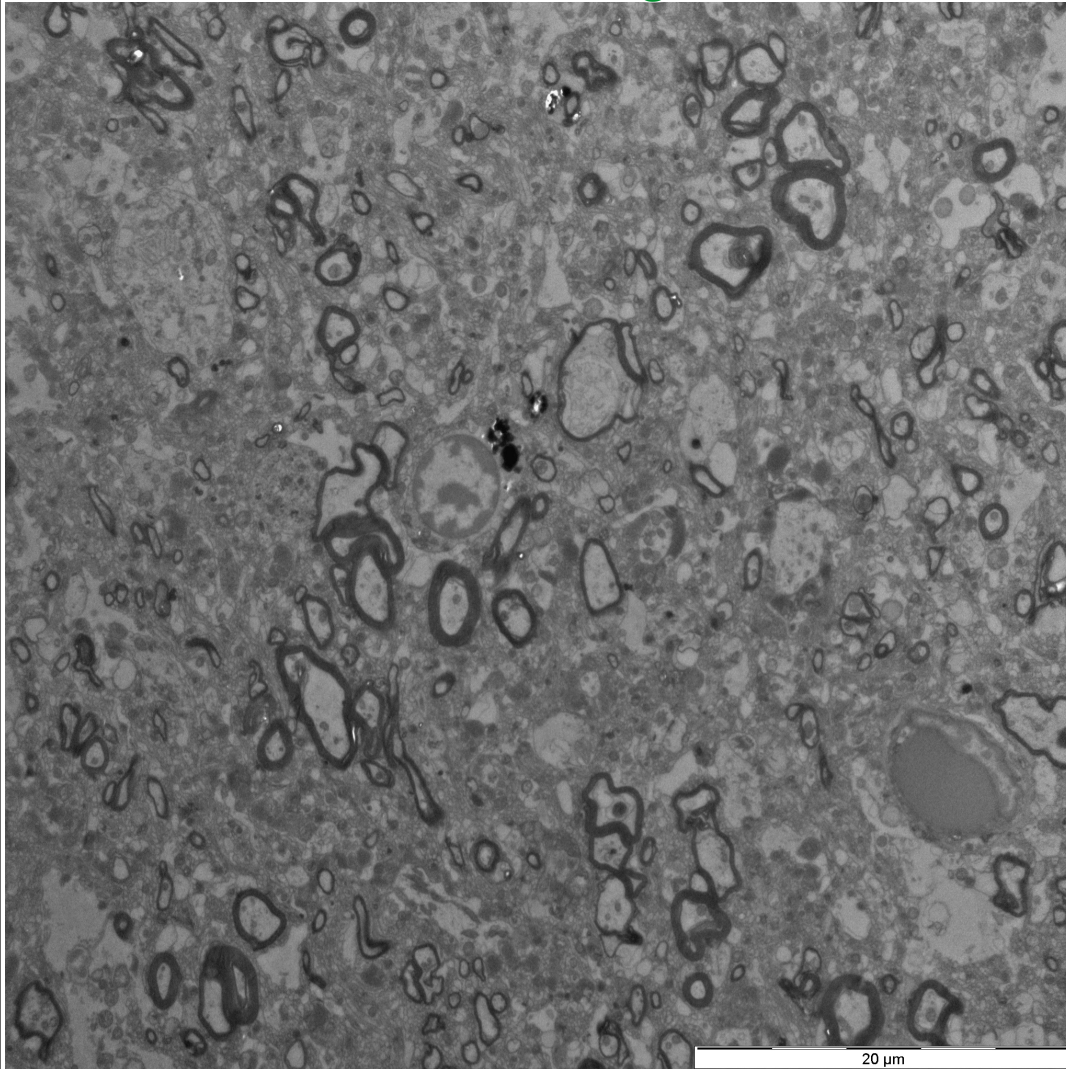
Electron Microscopy



Parkinson's Disease (PD)



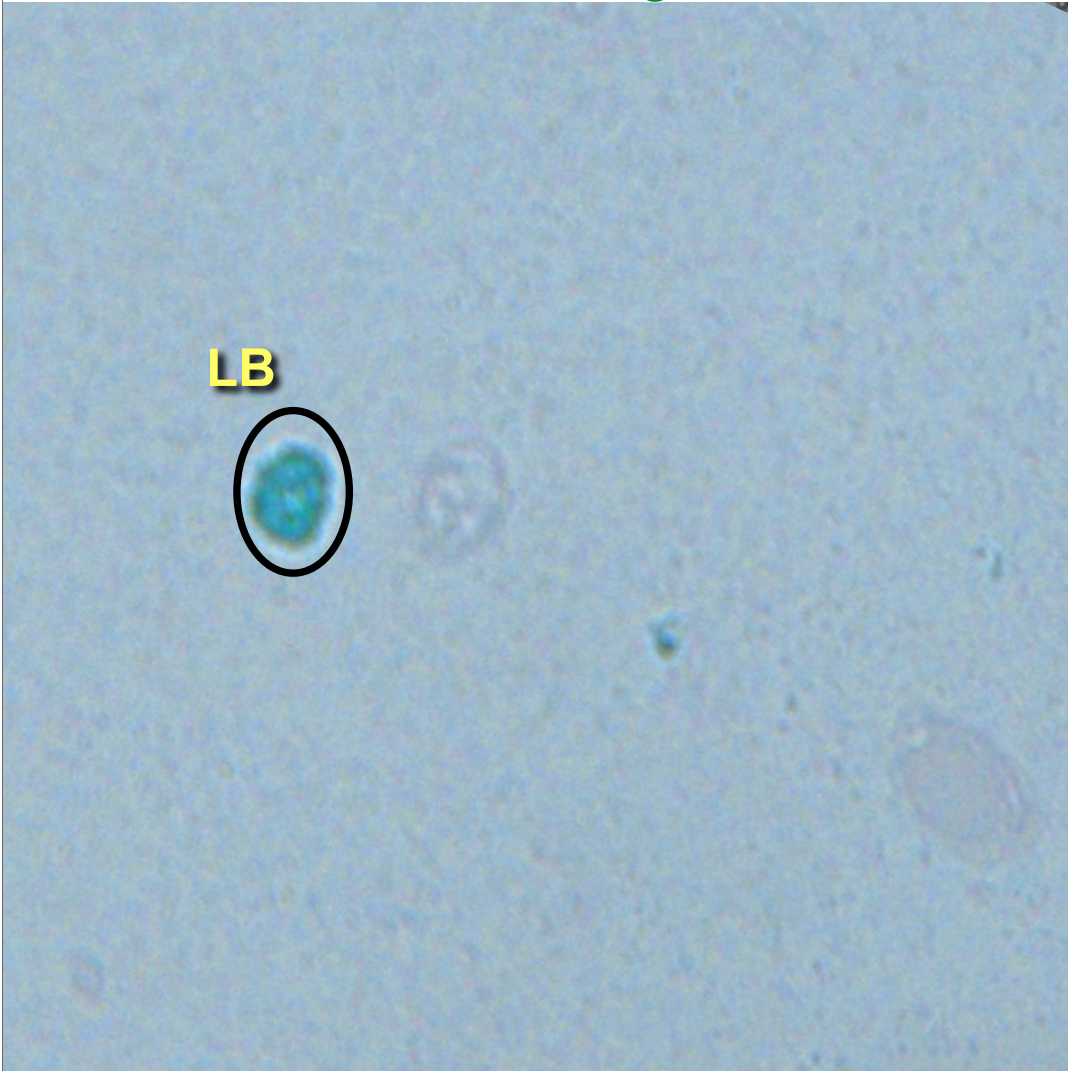
PD: CLEM - Correlative Light and Electron Microscopy



Parkinson's Disease (PD)

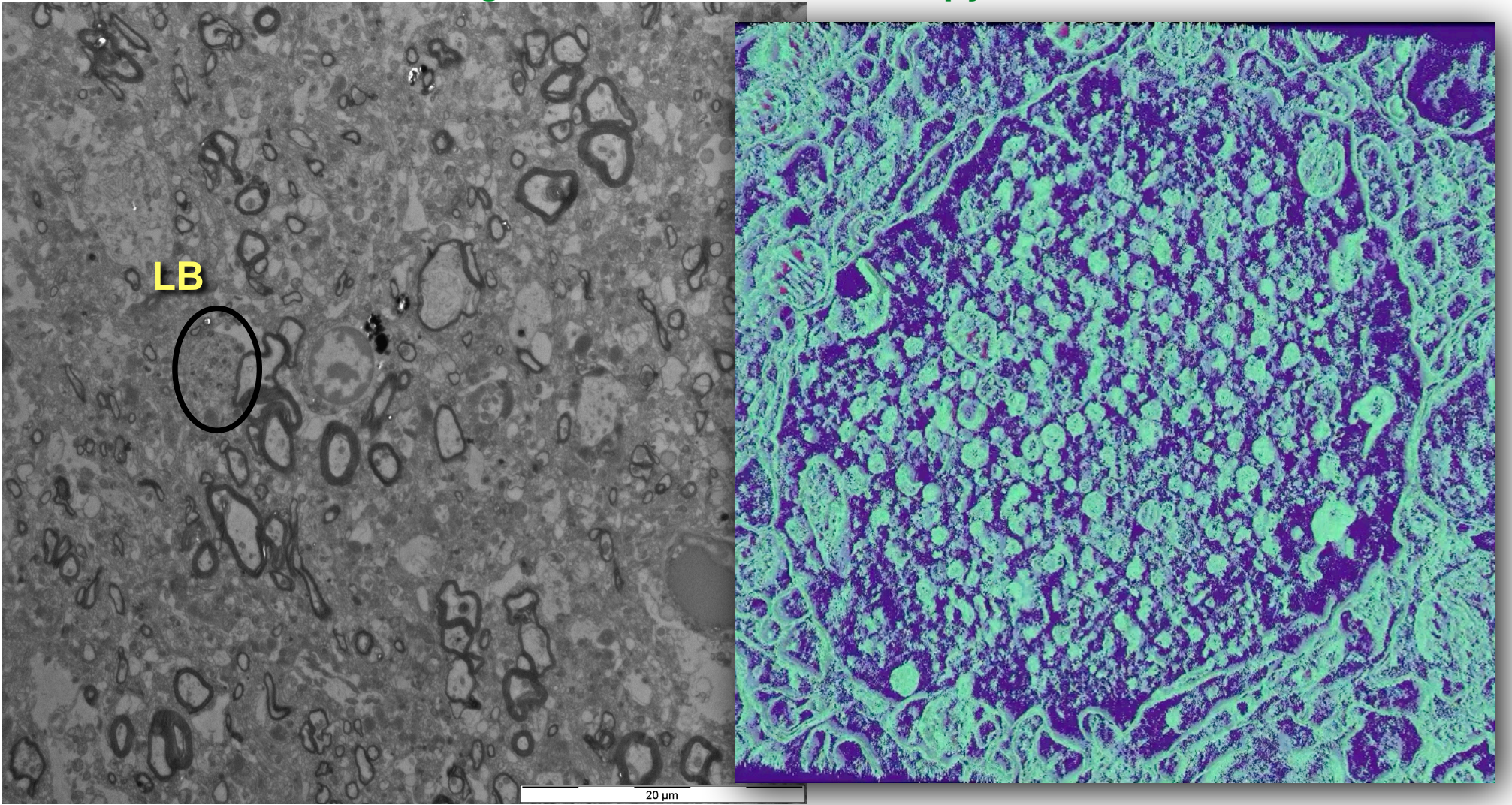
Shahmoradian *et al.*, Nature Neurosc. **22**, 1099-1109 (2019)

PD: CLEM - Correlative Light and Electron Microscopy



Shahmoradian *et al.*, Nature Neurosc. **22**, 1099-1109 (2019)

PD: CLEM - Correlative Light and Electron Microscopy



PD:

Lewy body, *Substantia nigra*

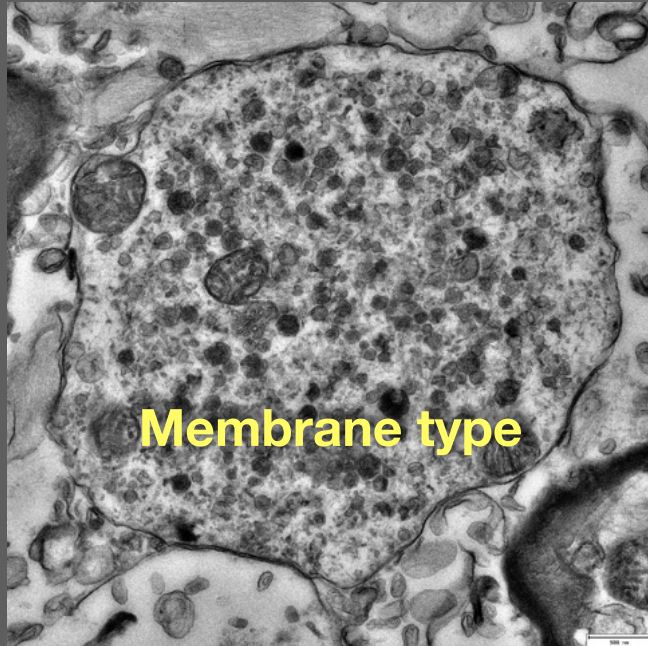
Amanda Lewis, LBEM



LB #1

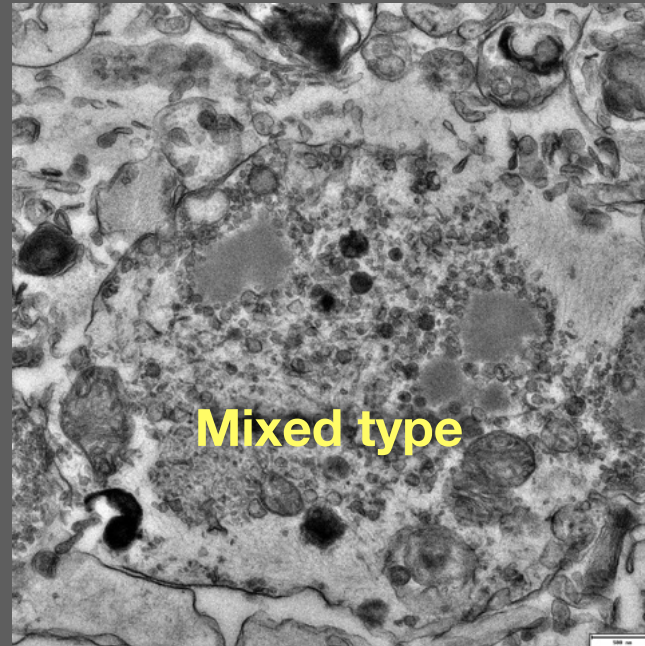
LB #2

LB #3



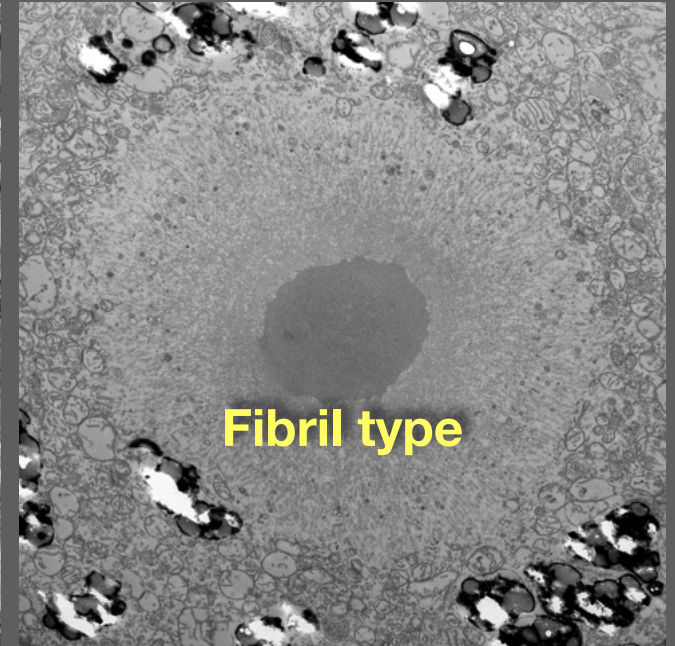
Membrane type

500 nm



Mixed type

500 nm



Fibril type

- organelles
- vesicles
- membranes
- filaments (peripheral+central, interspersed)
- dense granular regions

The majority of Lewy bodies in PD are primarily composed of membrane fragments

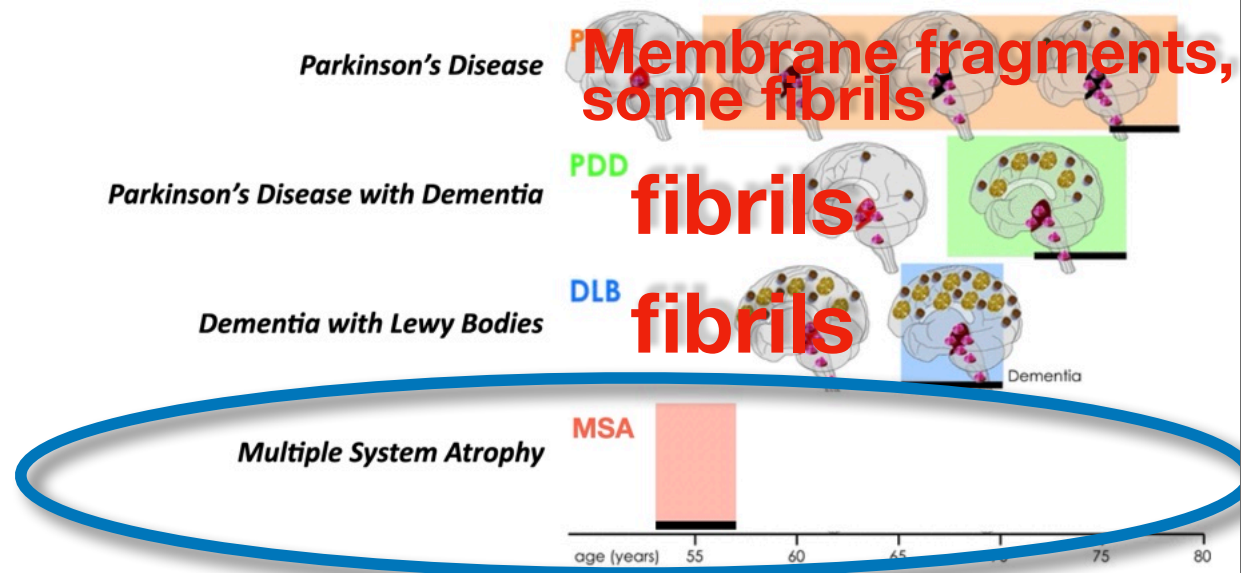
Shahmoradian *et al.*, *Nature Neurosc.* **22**, 1099-1109 (2019)

Lewis, AJ *et al* (2024) bioRxiv

Multiple System Atrophy (MSA)

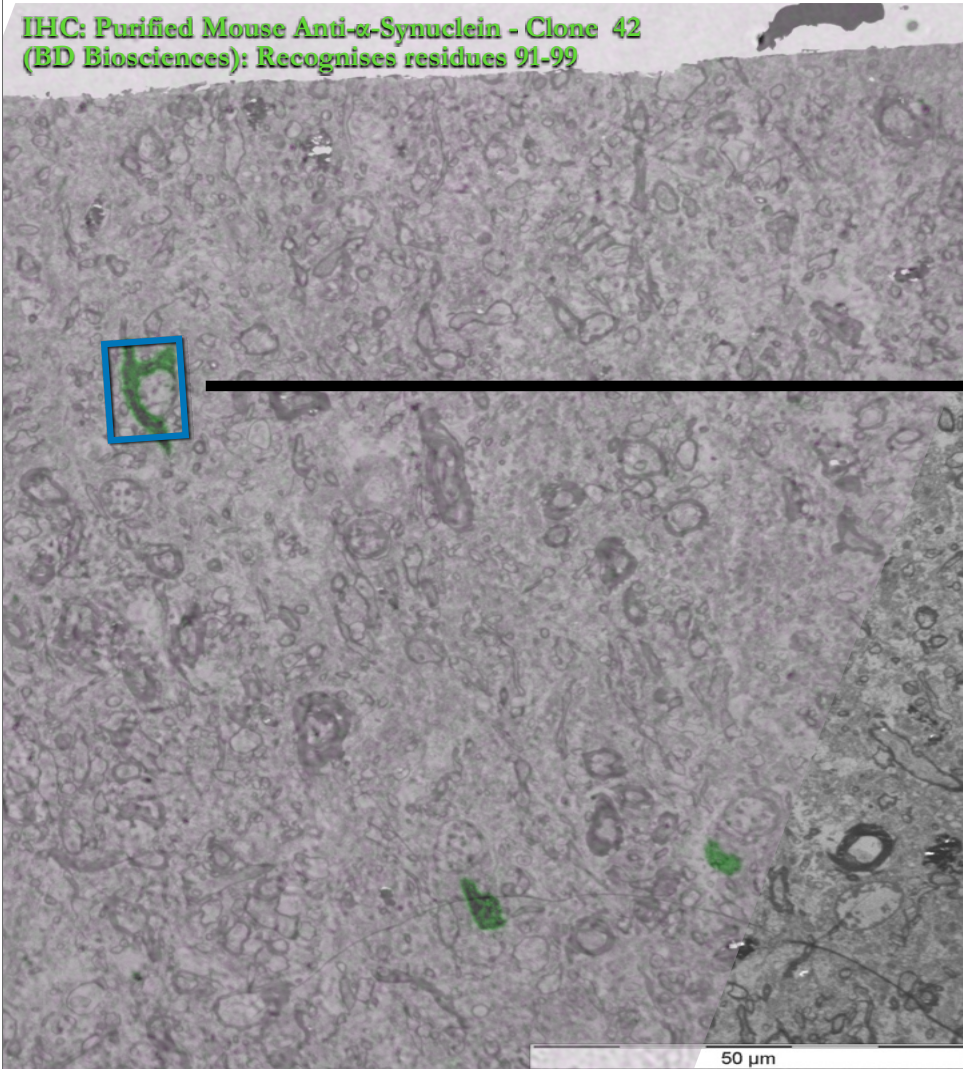


<https://www.multiplesystematrophy.org/>



MSA: *Substantia Nigra*

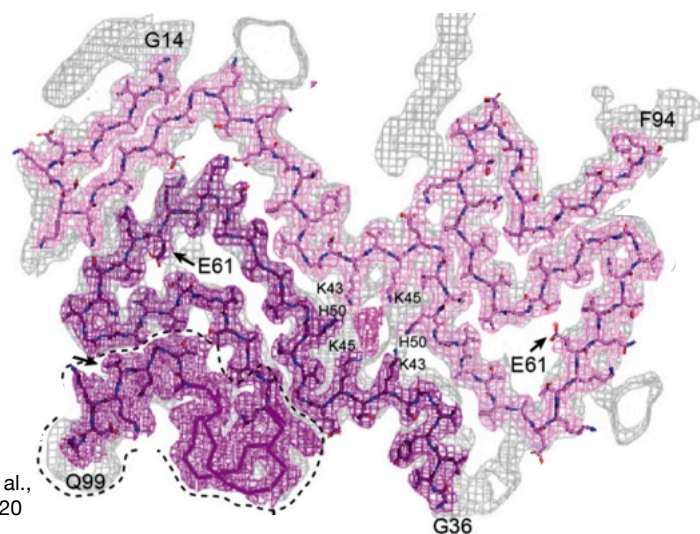
IHC: Purified Mouse Anti- α -Synuclein - Clone 42
(BD Biosciences): Recognises residues 91-99



Amanda Lewis, Domenic Burger, Carolin Böing

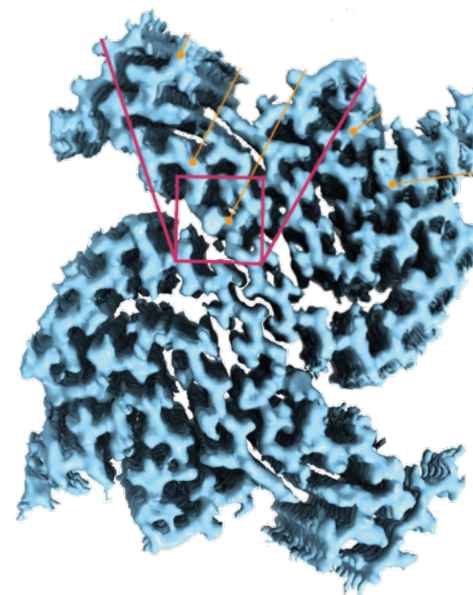


Multiple System Atrophy: A specific alpha-synuclein fibril strain



**Purified from human brain
of MSA patients**

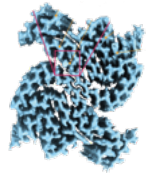
(Goedert and Scheres labs, MRC, Cambridge, UK)



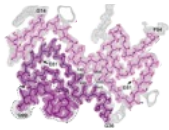
**Synthetic “1B” fibril,
causing MSA in mice**

(LBEM, collaboration with François Ichas, Bordeaux, France)

Multiple System Atrophy: A specific alpha-synuclein fibril strain

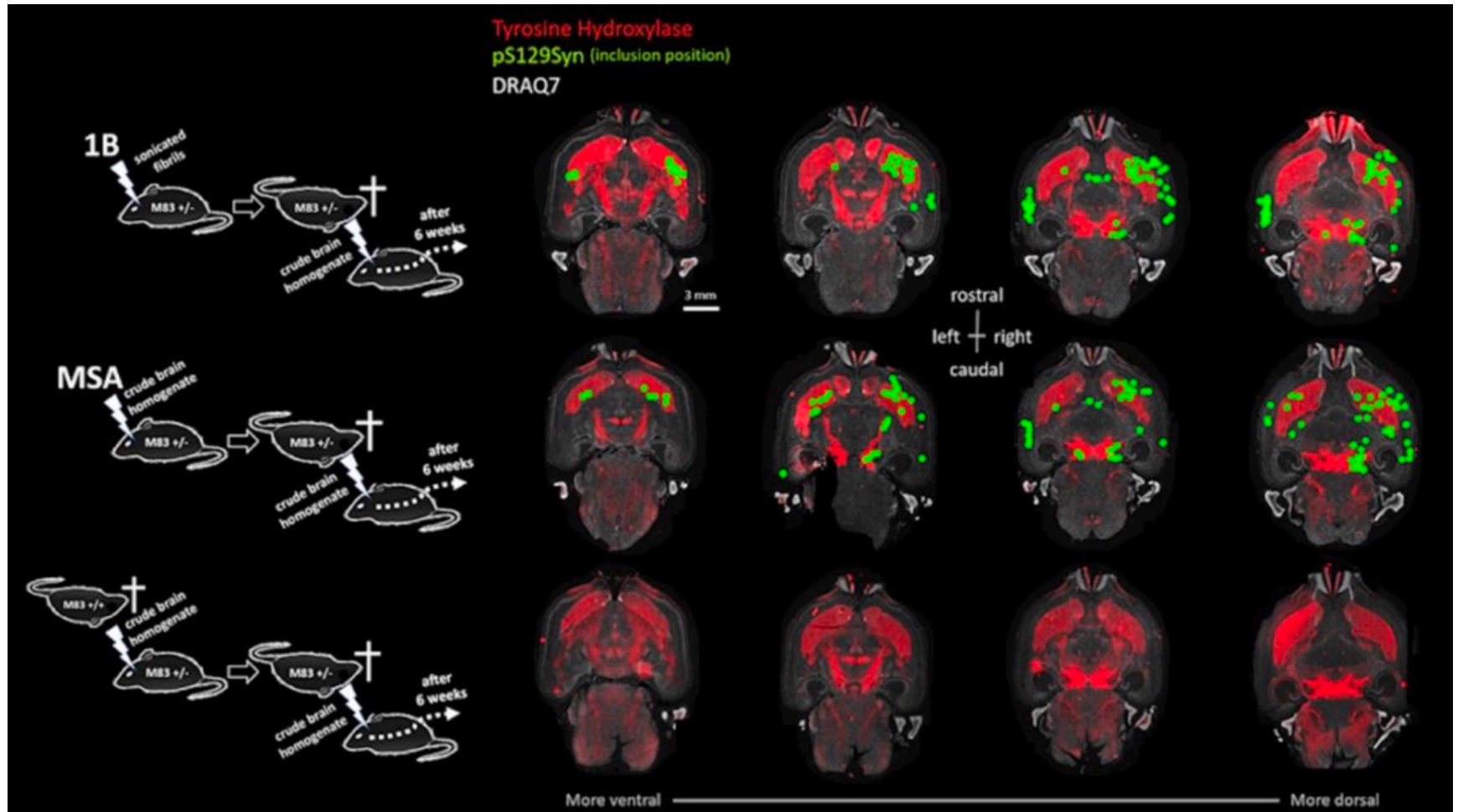


Synthetic "1B" fibril, causing MSA in mice

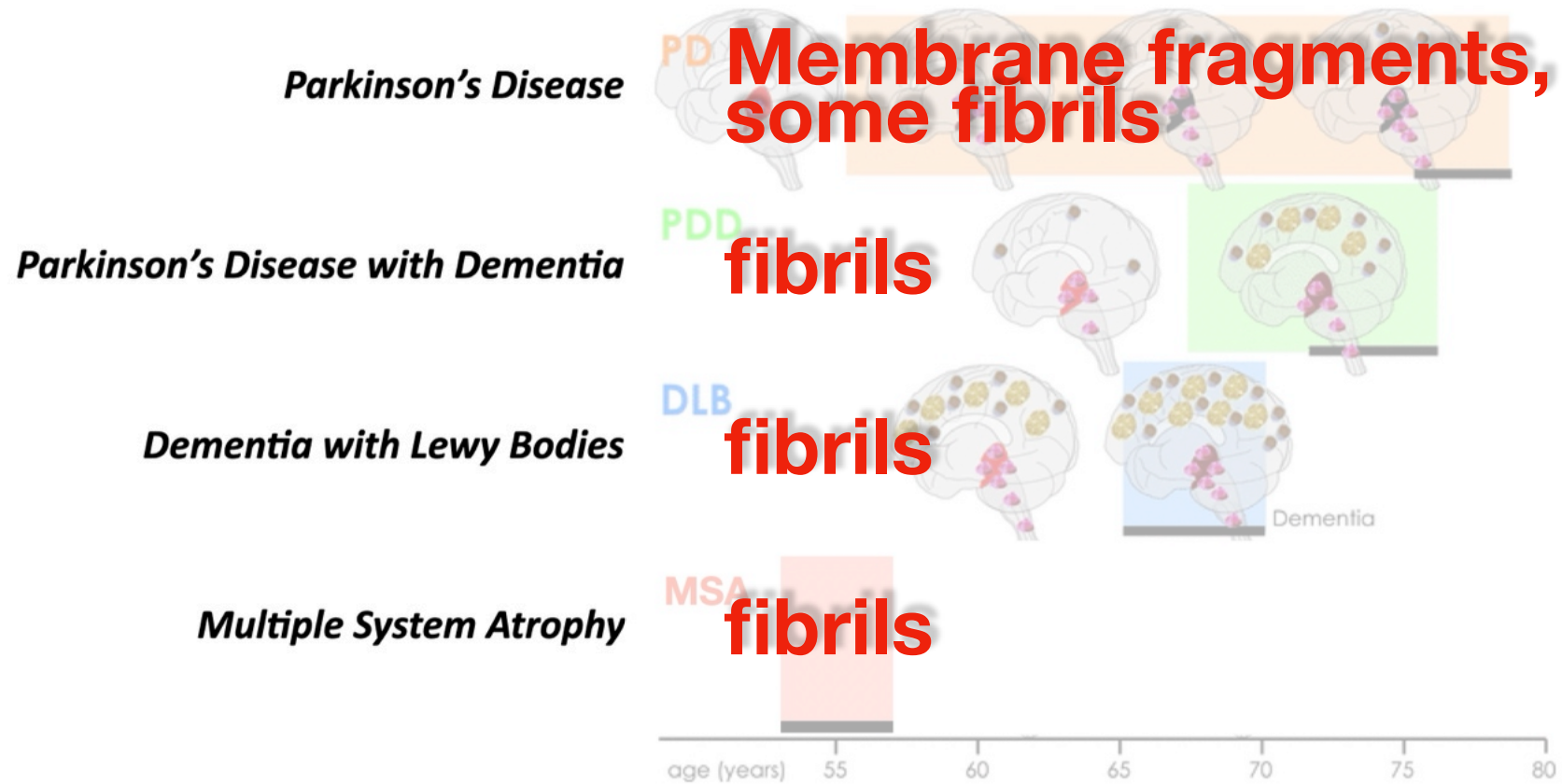


Purified from human brain of MSA patients

M83 mice express human A53T aSyn

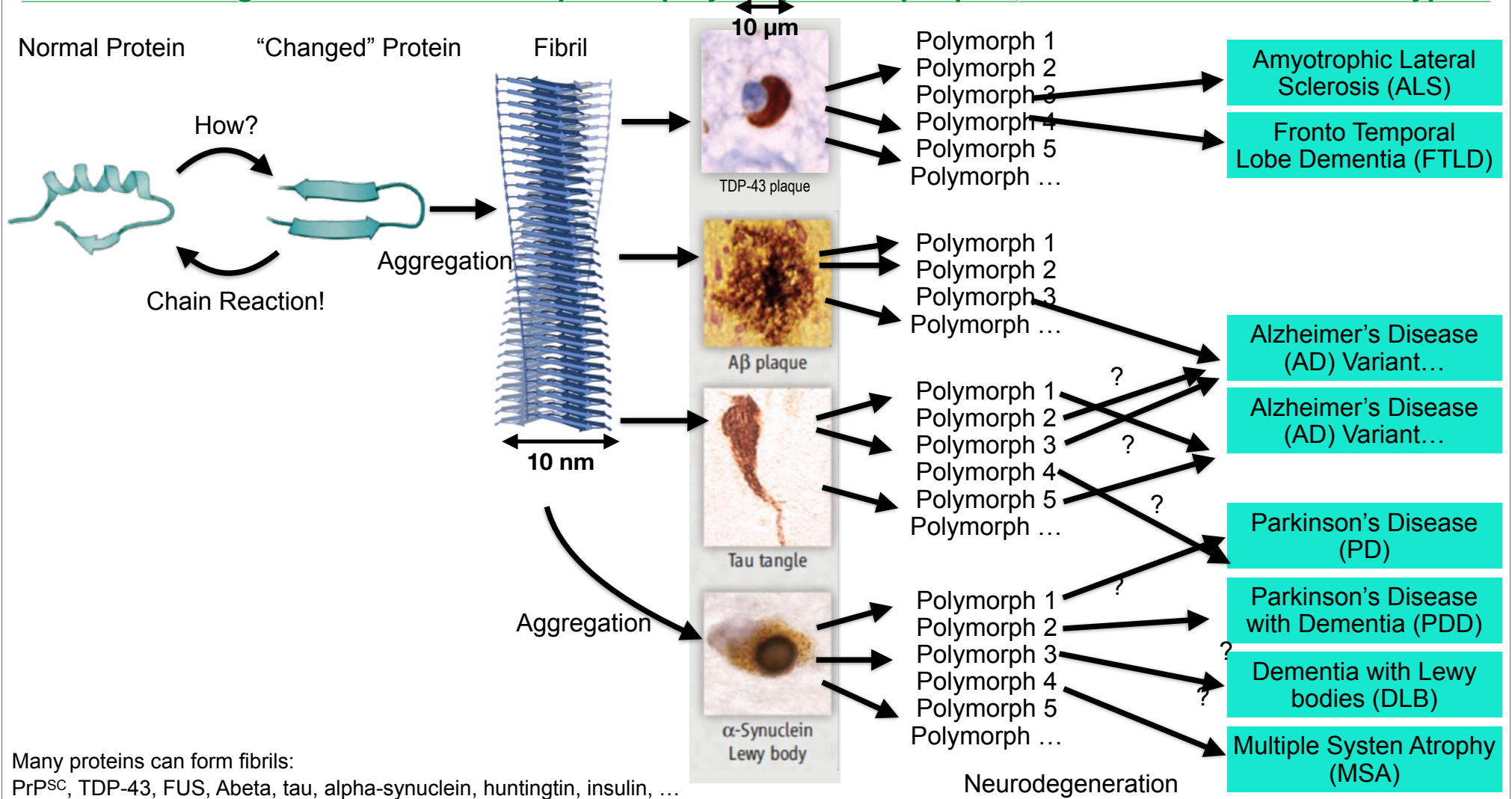


Synucleinopathies: Different “strains” of α -synuclein fibrils may cause different diseases

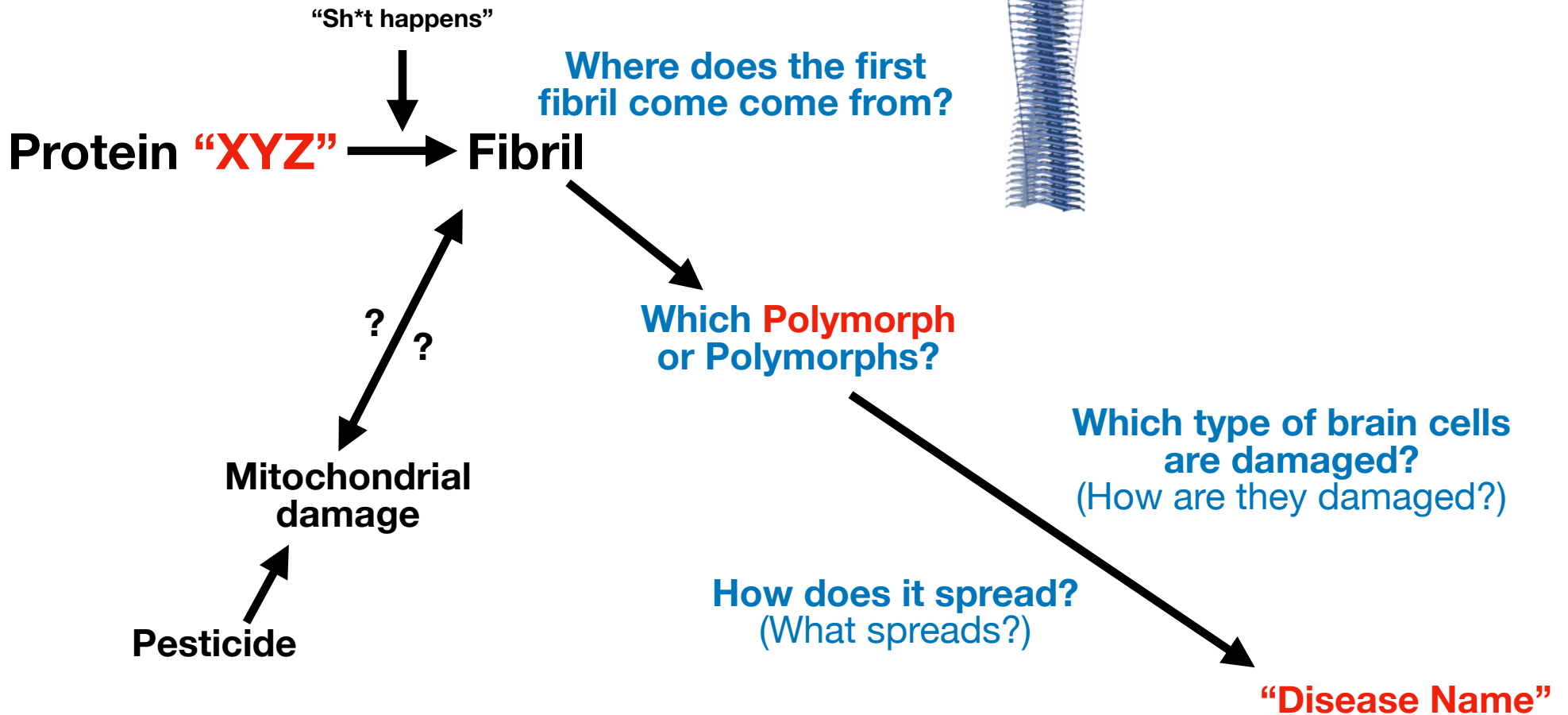


Modified from: Halliday & McCann, Annals of the New York Academy of Sciences 1184(1), 188-195 (2010)

Prionoid fibril growth: Fibrils of a specific polymorph form plaques, which cause disease sub-type?



Neurodegeneration: Alzheimer's, Parkinson's, DLB, PDD, MSA, ALS, FTL, Creutzfeldt-Jakob, ...



Benjamin Stecher: <https://tmrwedition.com/>

Structural Investigations of Neurodegeneration

Biology: Parkinson's Disease



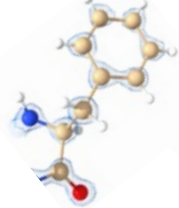
**We need more “contrast” in
cryo-Electron Microscopy.**

Dubochet Center for Imaging Lausanne: Apoferritin @ 1.09 (March 2024)

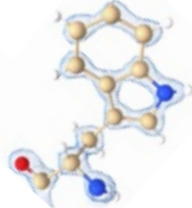


EMPIAR: 11866
EMDB: 19436
PDB: 8RQB

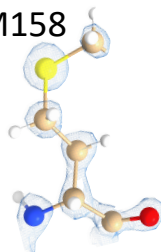
F51



W93



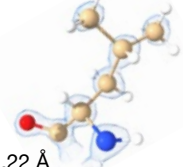
M158



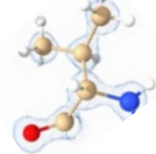
C130



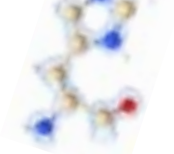
L155



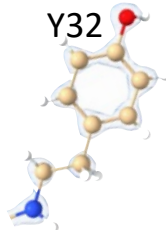
V33



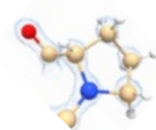
H118



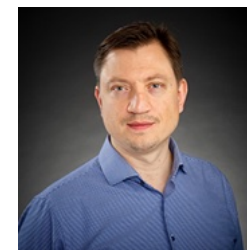
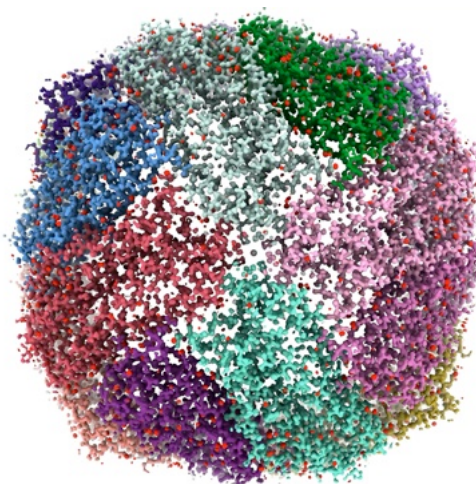
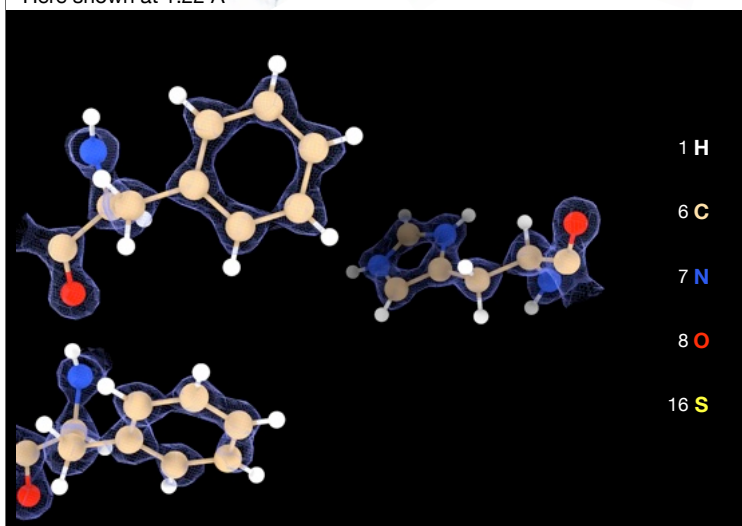
Y32



P127



Here shown at 1.22 Å



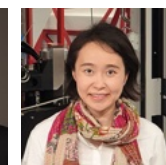
Alex Myasnikov
Technical Director



Christel Genoud
Executive Director



Bertrand
Beckert



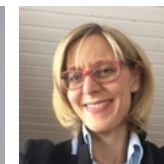
Emiko
Uchikawa



Inay
Mohamed



Sergey
Nazarov



Mireille
Fasmeyer

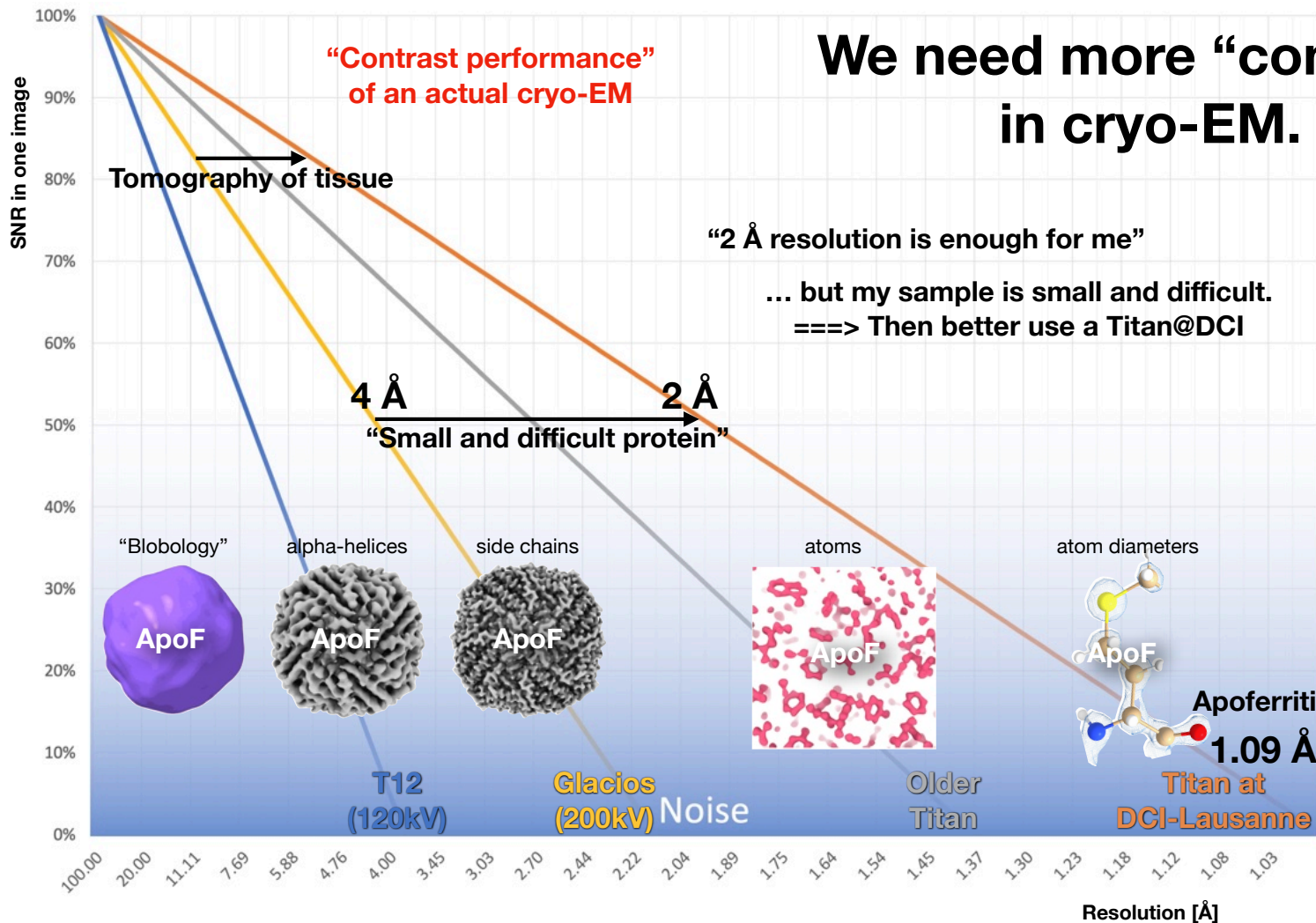


Florent
Wenger



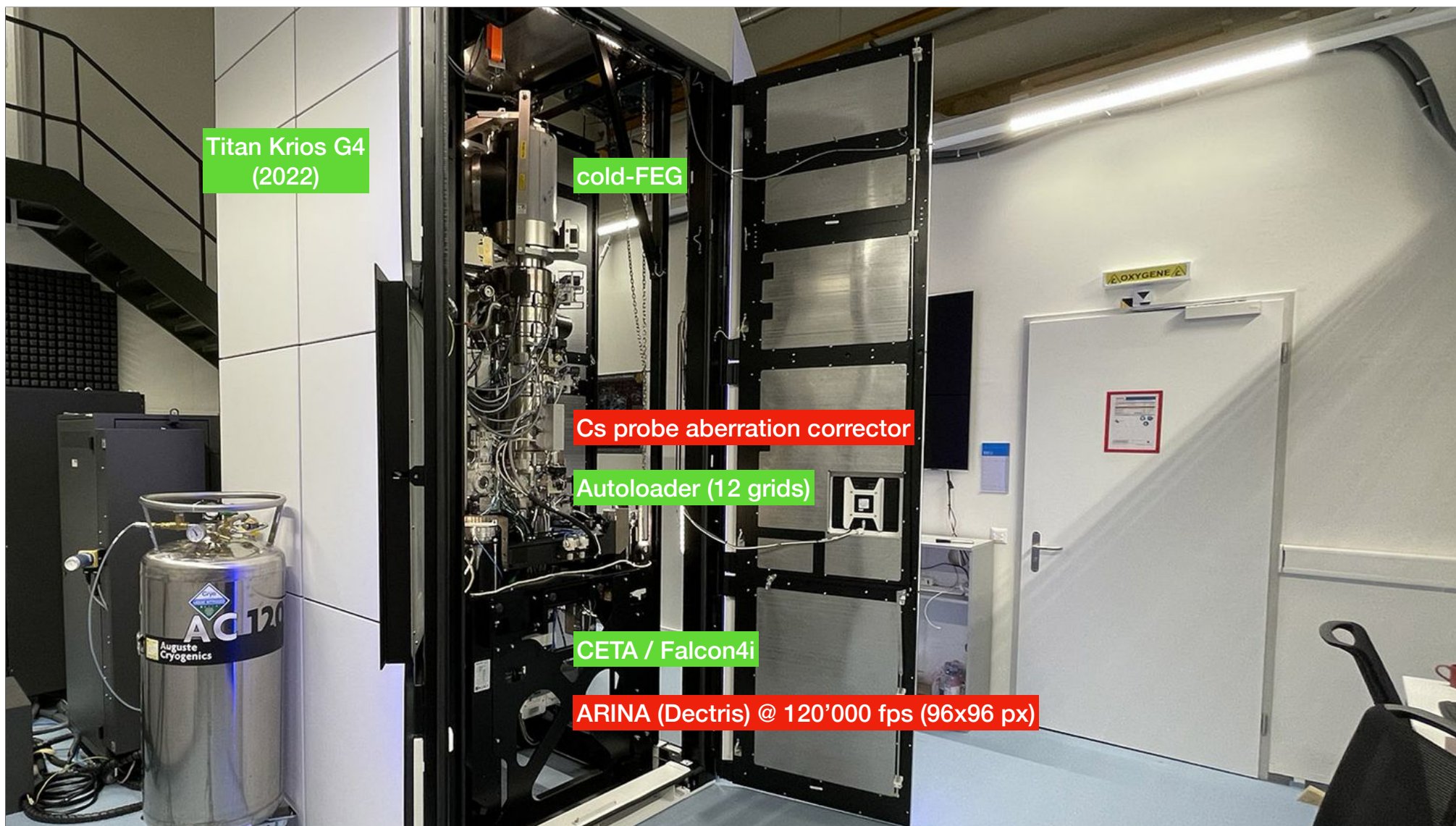
Sofya
Laskina

High resolution is essential, even if you don't need it.



EMPIAR: 11866
 EMDDB: 19436
 PDB: 8RQB

**We need more “contrast”
in cryo-EM.**



Titan Krios G4
(2022)

cold-FEG

Cs probe aberration corrector

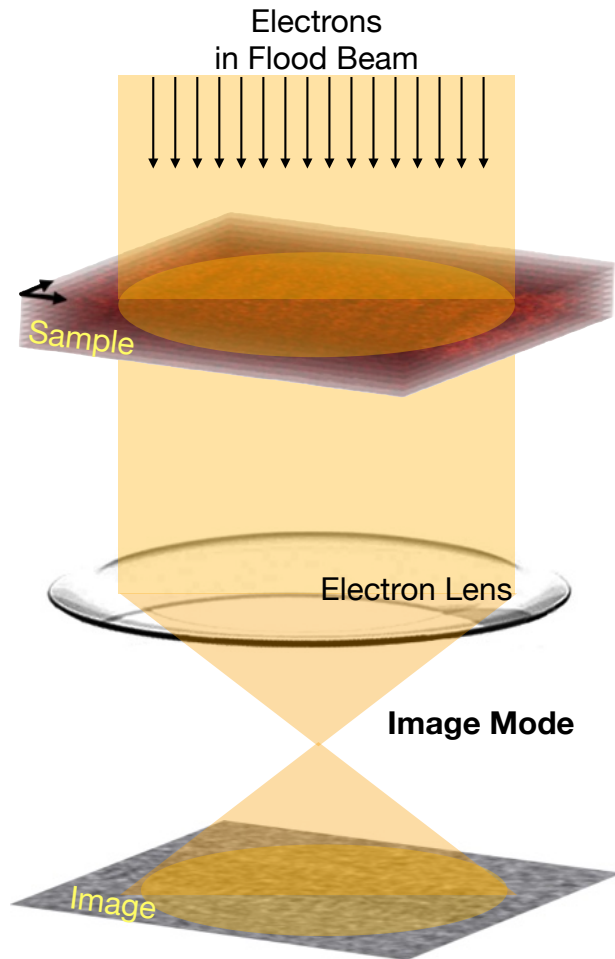
Autoloader (12 grids)

CETA / Falcon4i

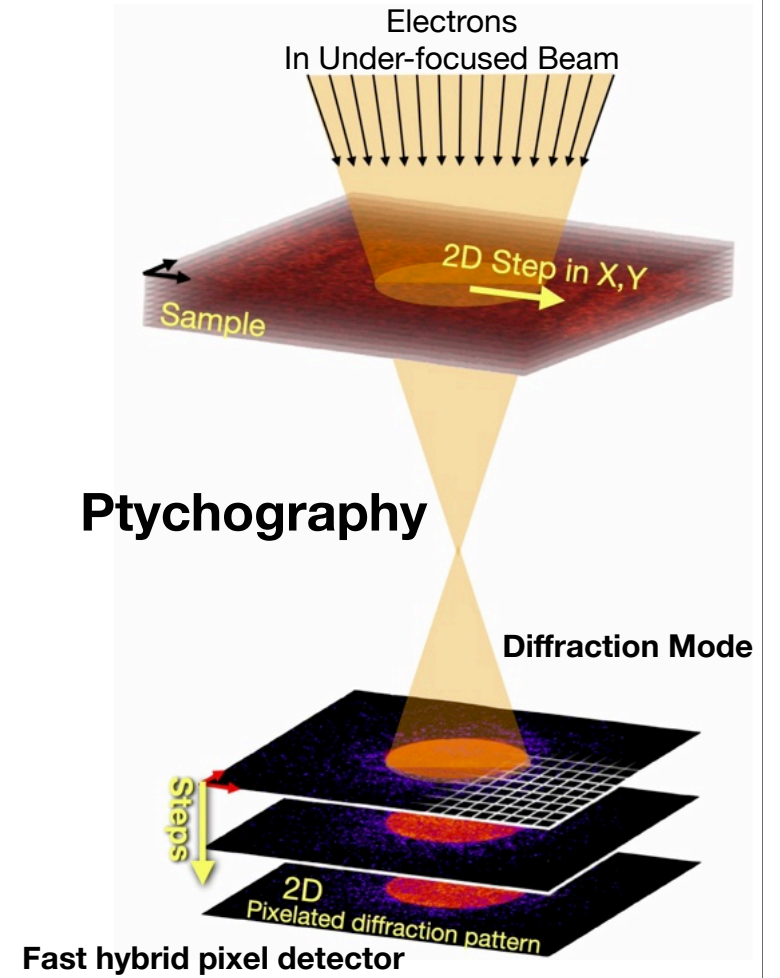
ARINA (Dectris) @ 120'000 fps (96x96 px)

Cryo-Electron Microscopy of Proteins

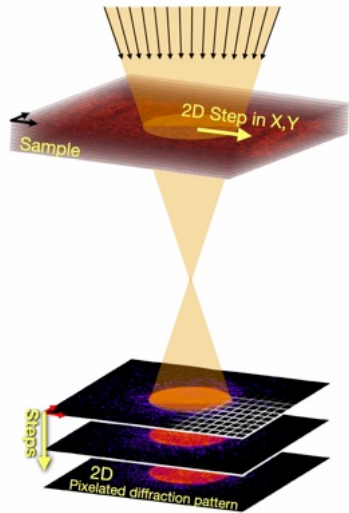
Cryo-TEM



4D-STEM



4D-STEM: Parallax (TcBF) vs. Ptychography reconstruction

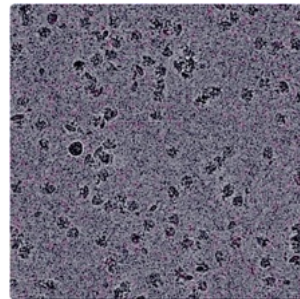
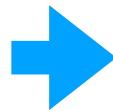
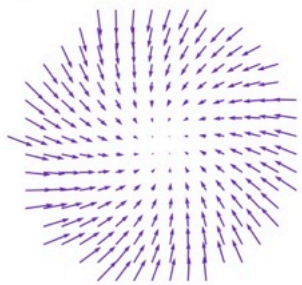


512 x 512 beam positions
= 262'144 beam positions

= 2.4 GB
@ 120'000 fps => 2 seconds

96 x 96 pixels on detector
(262'144 diffraction patterns)

Parallax



Images are aligned to each other and averaged

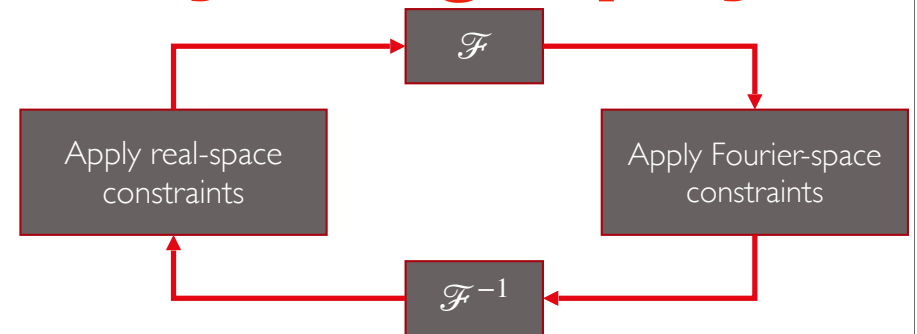
py4Dstem

axXiv:2309.05250v1 (2023)

Iterative Phase Retrieval Algorithms for Scanning Transmission Electron Microscopy

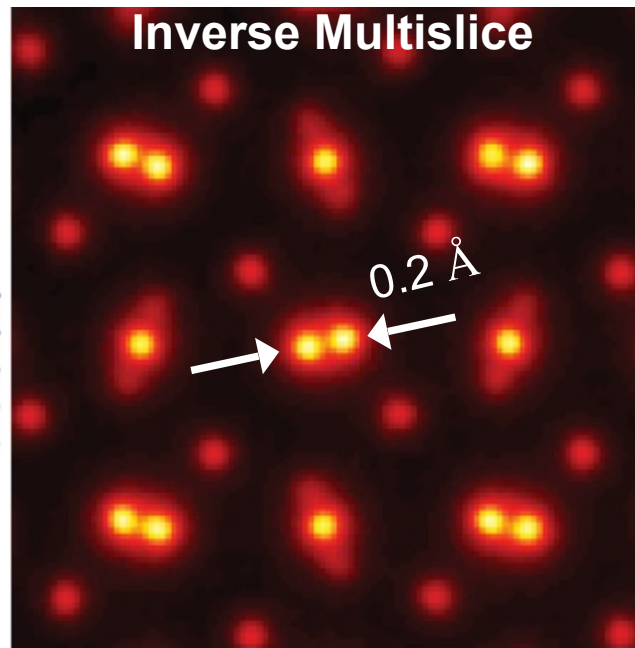
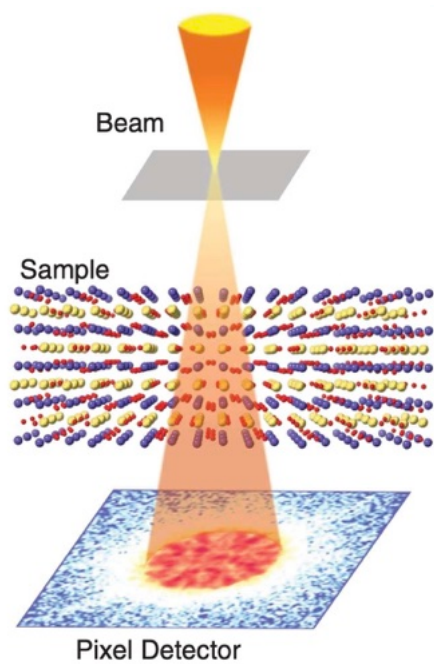
GEORGIOS VARNAVIDES,^{1,2,†} STEPHANIE M. RIBET,^{2,3,4,†} STEVEN E. ZELTMANN,^{5,6} YUE YU,^{7,8} BENJAMIN H. SAVITZKY,² VINAYAK P. DRAVID,^{3,4,9} MARY C. SCOTT,^{2,5} AND COLIN OPHUS^{2,†}

Ptychography



4D STEM in Materials Sciences: Ptychography

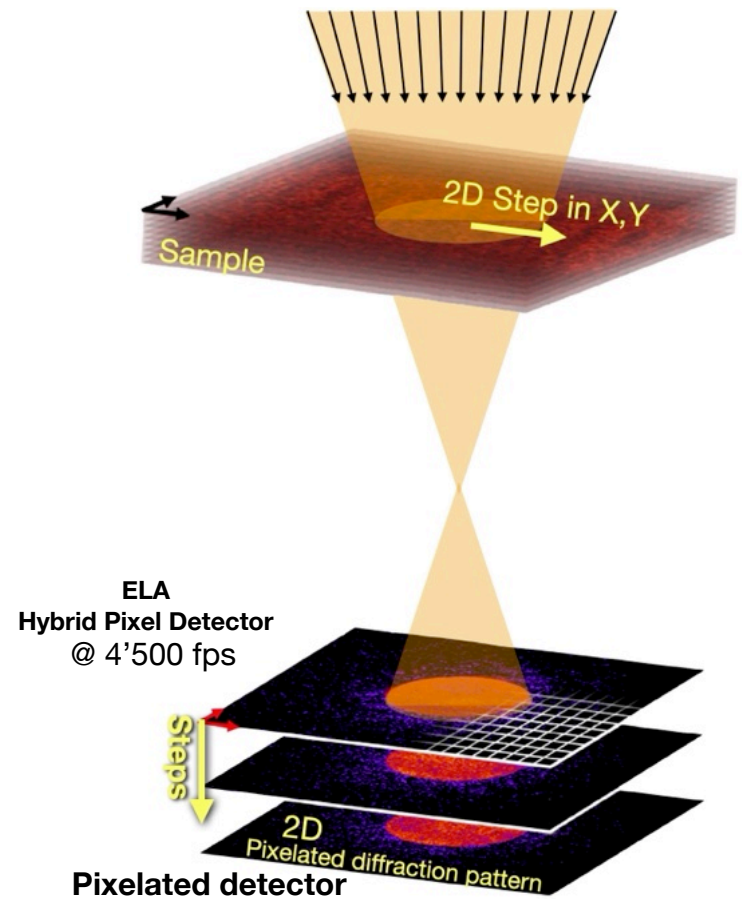
Resolution of 0.2 Å



Chen, ..., Muller:
Science 2021

4D STEM (Ptychography)

Electrons
In Under-focused Beam



4D STEM

B. Küçükoğlu et al., (2024) [bioRxiv.org](https://doi.org/10.1101/2024.02.12.579607) 2024.02.12.579607

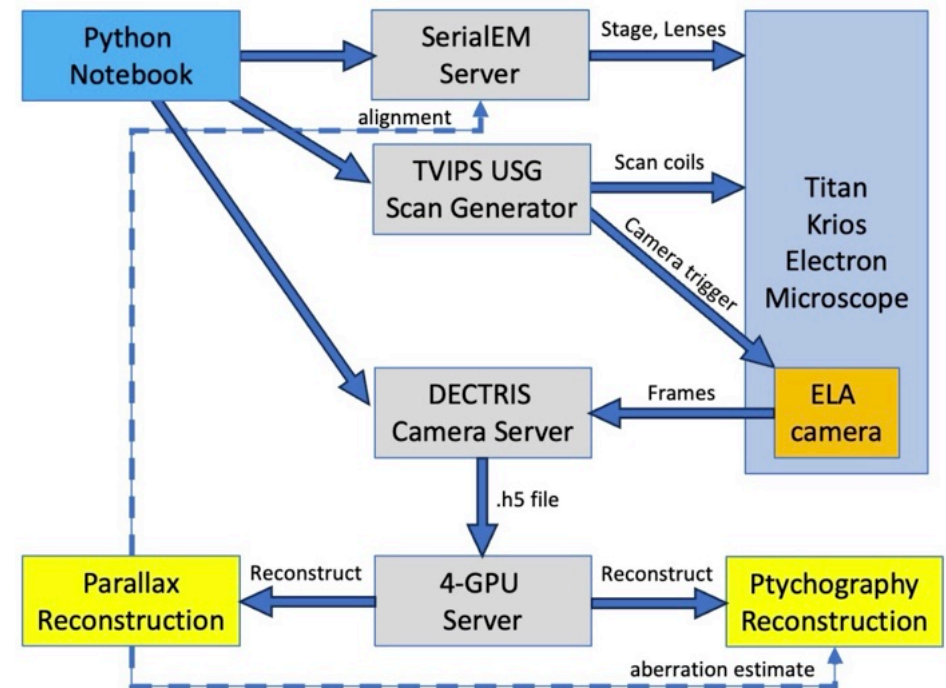
80% overlap in X and Y

512 x 512 positions

96 x 96 px / frame

2 GB raw data per scan

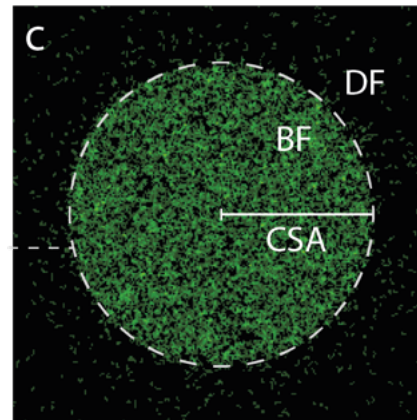
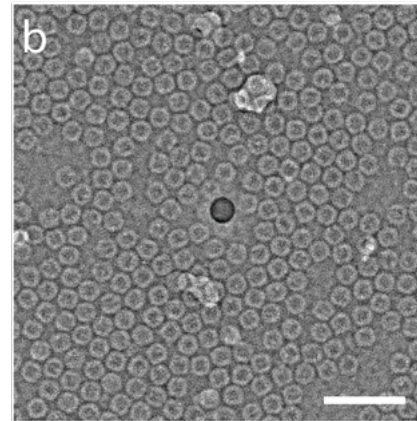
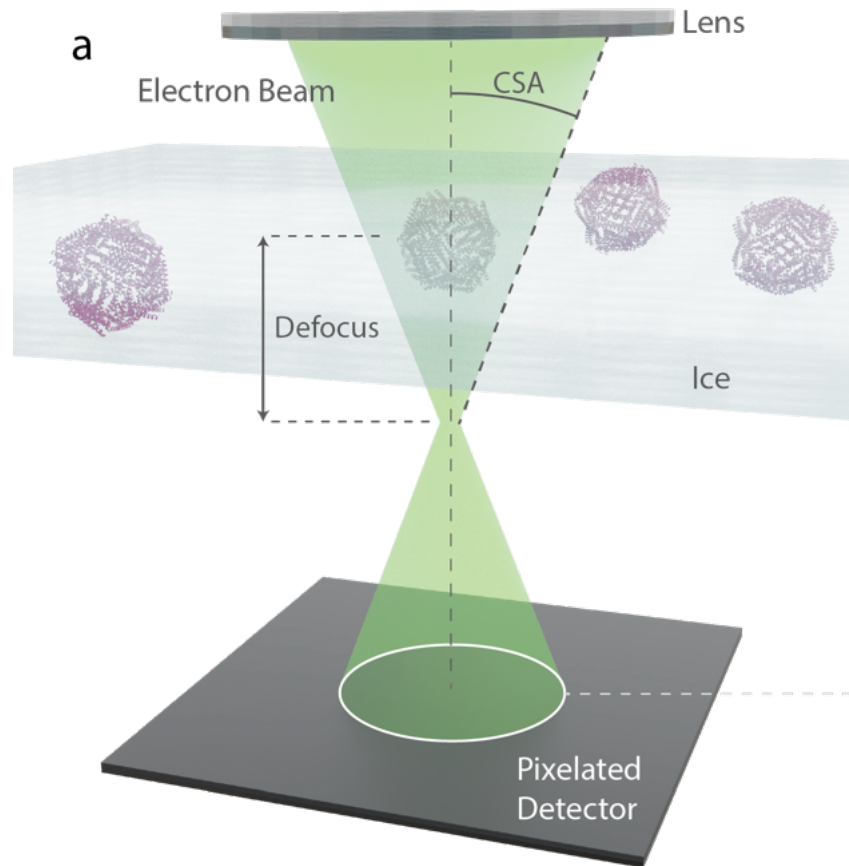
5 e⁻/Å² total fluency



Thanks for help with SerialEM integration from Michael Elbaum and Shahar Seifer, Weizmann, Israel

4D STEM

B. Küçüköğlü et al., (2024) [bioRxiv.org](https://doi.org/10.1101/2024.02.12.579607) 2024.02.12.579607



(Sum of 3 recorded frames)
CSA = 4 mrad

Titan Krios G4:

- 300kV cold-FEG
- Probe correction $C_s=0\text{mm}$
- TVIPS USG
- ELA detector

Illumination:

- CSA: 4.0 to 6.0 mrad
- Defocus: 1.0 to 2.0 μm
- Beam diameter: 8 to 24 nm

Low-dose conditions:

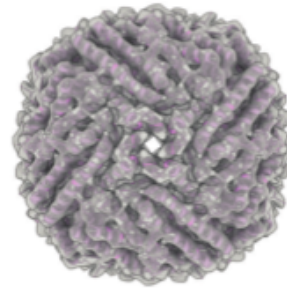
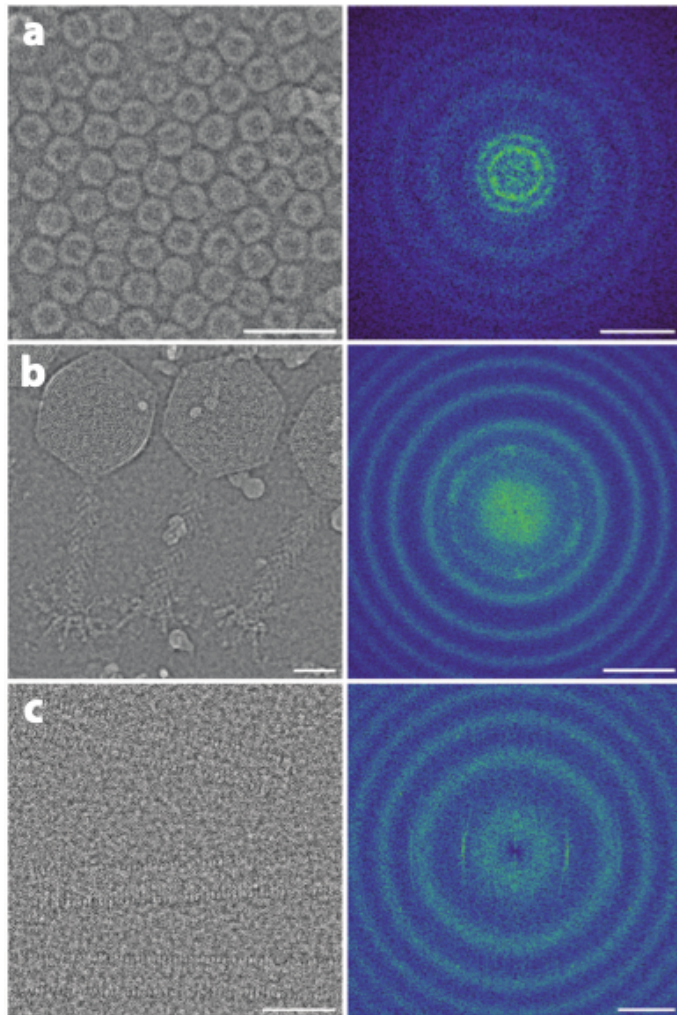
- 35...50 $\text{e}^-/\text{\AA}^2$

Specimens:

- Apoferritin
- Phi92 Bacteriophage
- Tobacco Mosaic Virus
- Bacteriorhodopsin 2D crystals

Cryo-electron ptychography of proteins

B. Küçüköğlü et al., (2024) [bioRxiv.org](https://doi.org/10.1101/2024.02.12.579607) 2024.02.12.579607



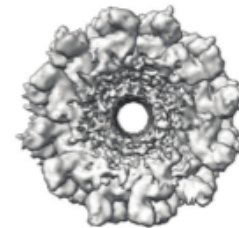
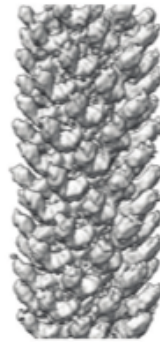
Apoferritin

CSA: 4.0 mrad

Dose: 35e-/Å²

Number particles: 11'552

Final Resolution: 5.8 Å



Phi92 stalk

CSA: 5.1 mrad

Dose: 49e-/Å²

Number particles: 1'600

Final Resolution: 8.4 Å



TMV

CSA: 6.1 mrad

Dose: 32e-/Å²

Number particles: 2'120

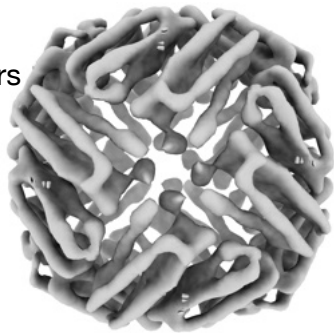
Final Resolution: 6.4 Å

Cryo-electron ptychography

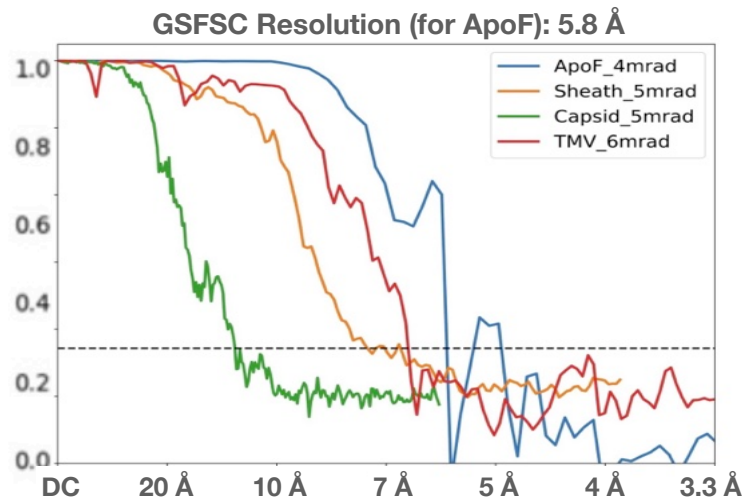
ToDo:

- Dose fractionation
- Motion correction
- Dose-dep. resolution filters

- Larger CSA
- Less defocus
- Multi-slice reconstruction



Titan Krios G4, Probe Corrector, ELA: 11'552 particles



vs. Cryo-EM

Implemented:

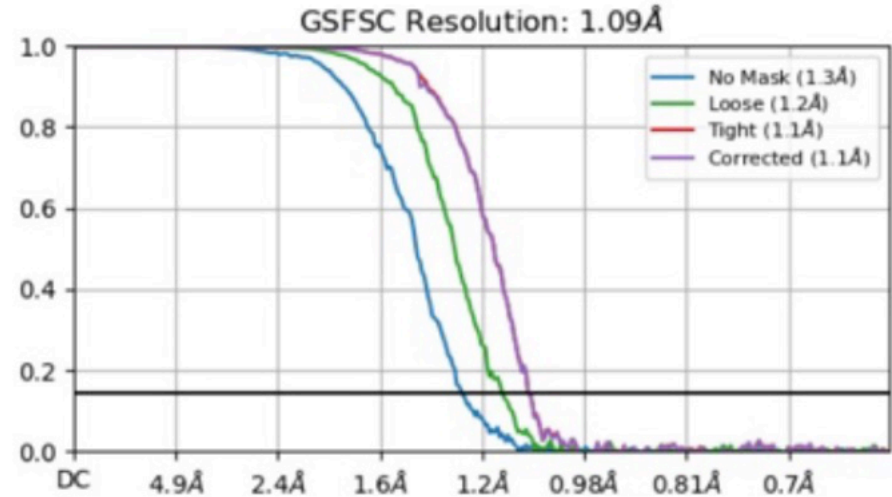
- Dose fractionation
- Motion correction
- Dose-dep. resolution filters



Alex Myasnikov
Inay Mohammed
Sergey Nazarov

EMPIAR: 11866
EMDB: 19436
PDB: 8RQB

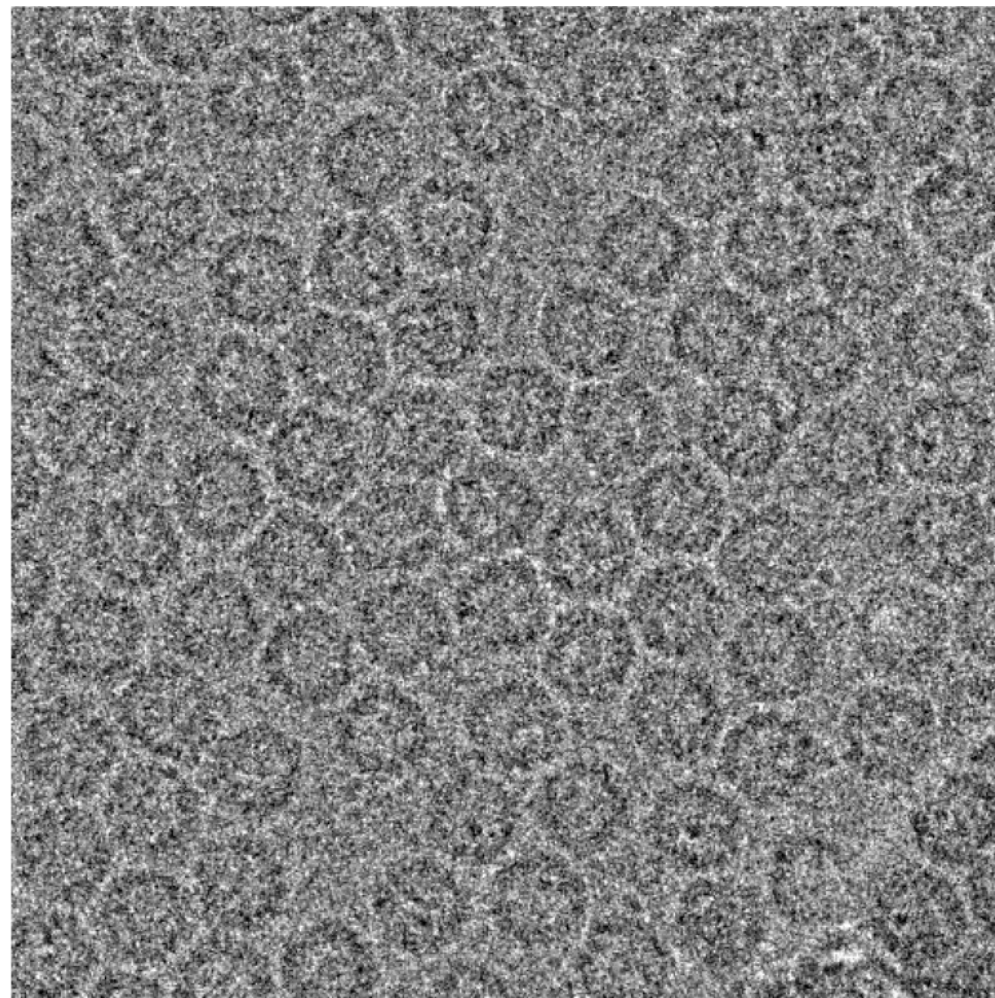
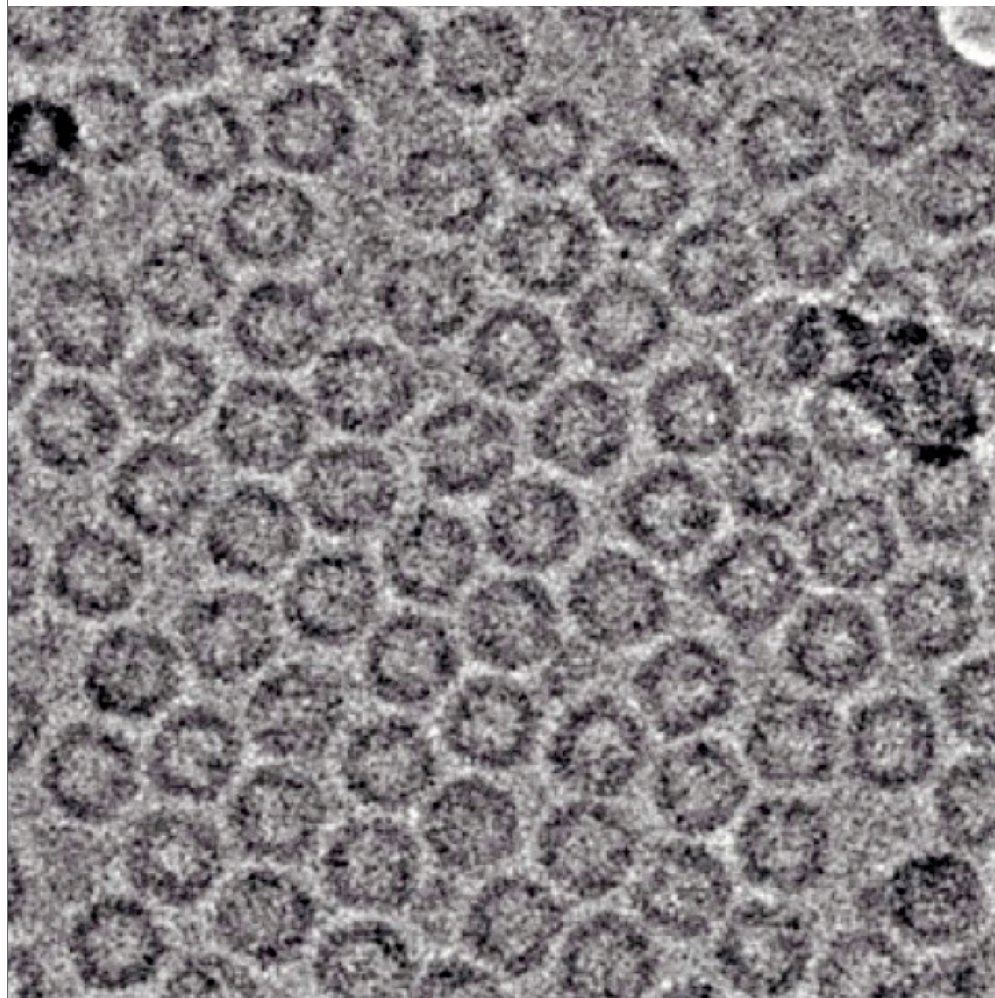
Titan Krios G4, Falcon4i: 411'705 particles



Cryo-electron ptychography

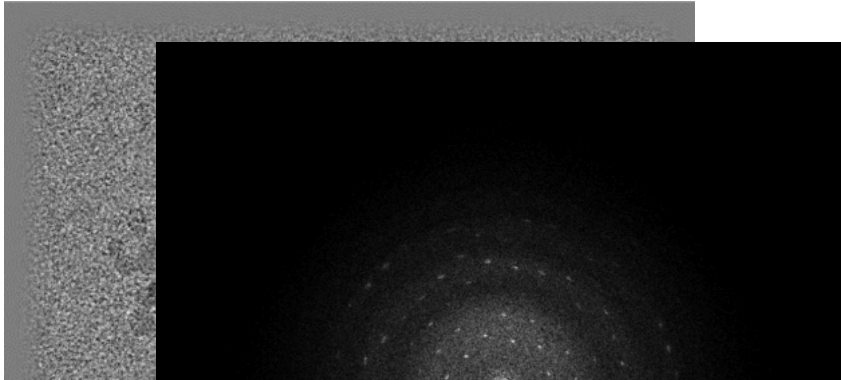
vs.

Cryo-EM

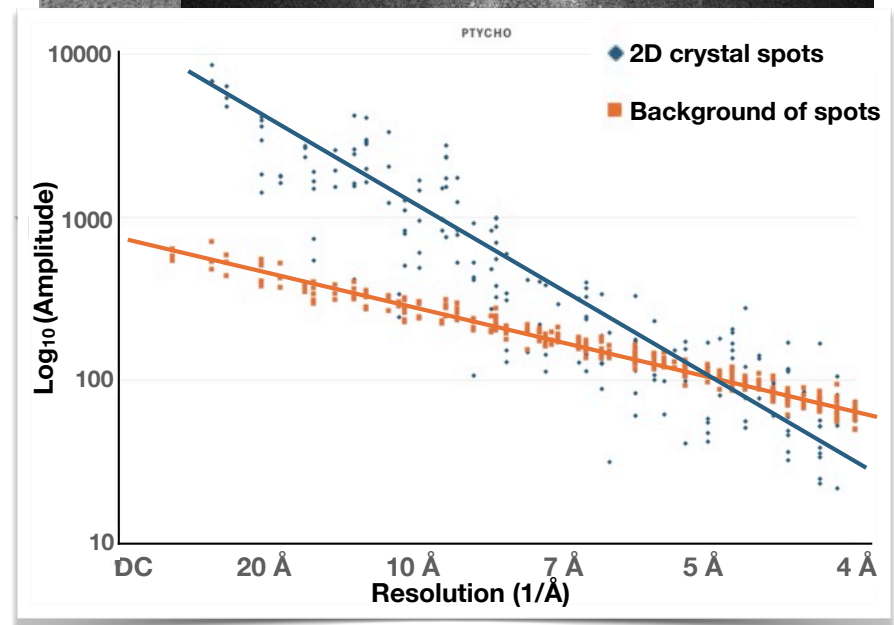
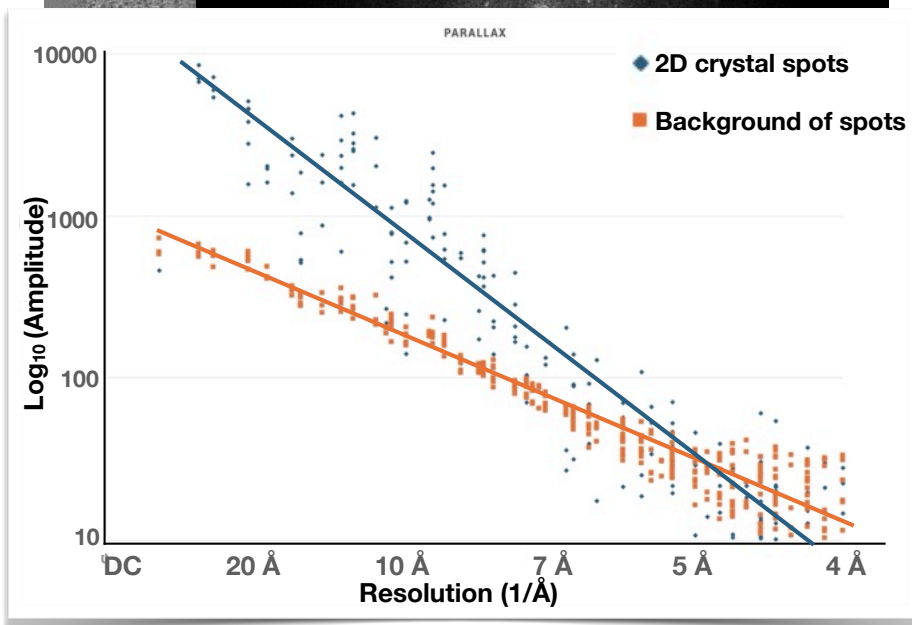
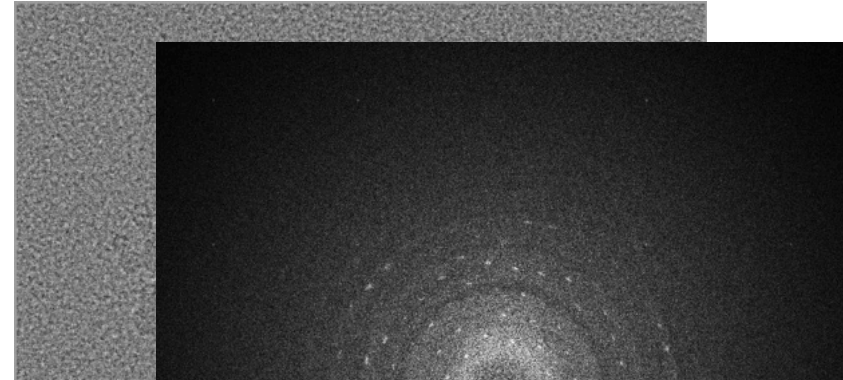


Cryo-electron ptychography of Bacteriorhodopsin 2D crystals

Parallax Reconstruction (py4Dstem)

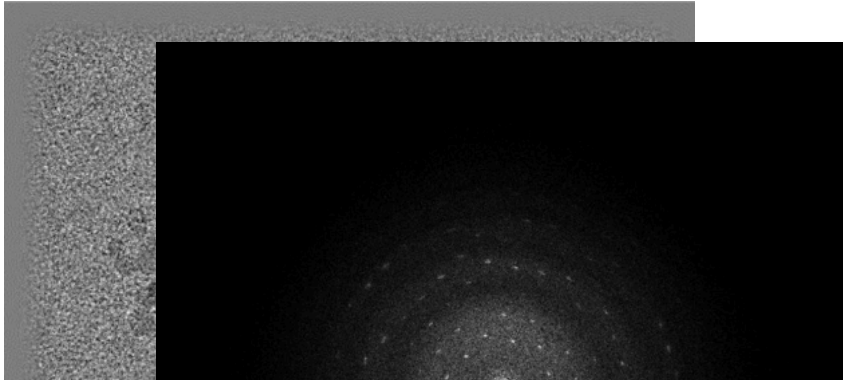


Ptychography Reconstruction (py4Dstem)

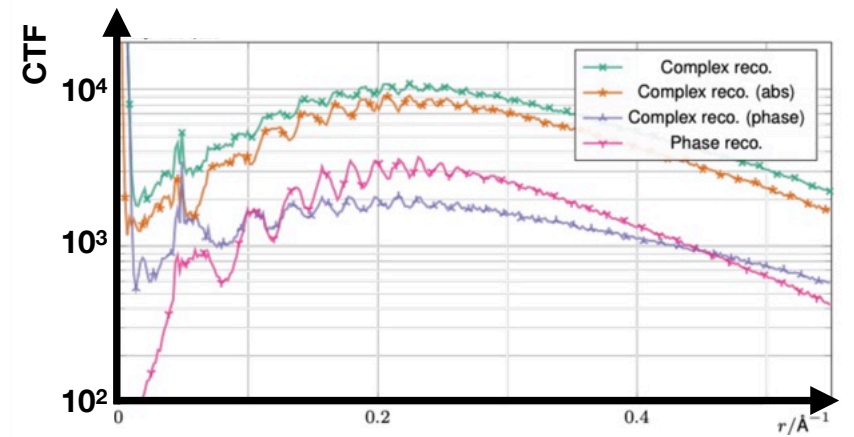
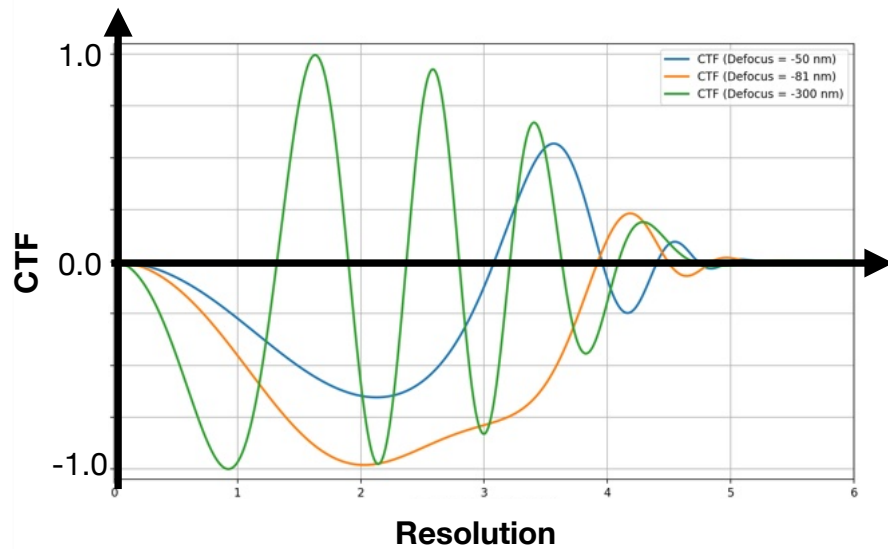
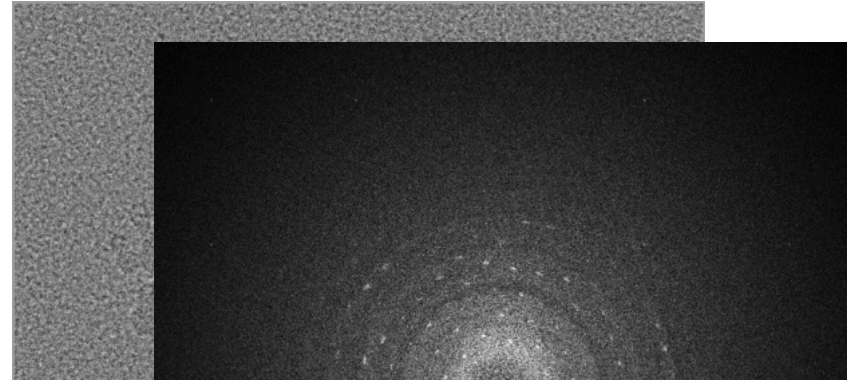


Cryo-electron ptychography of Bacteriorhodopsin 2D crystals

Parallax Reconstruction (py4Dstem)

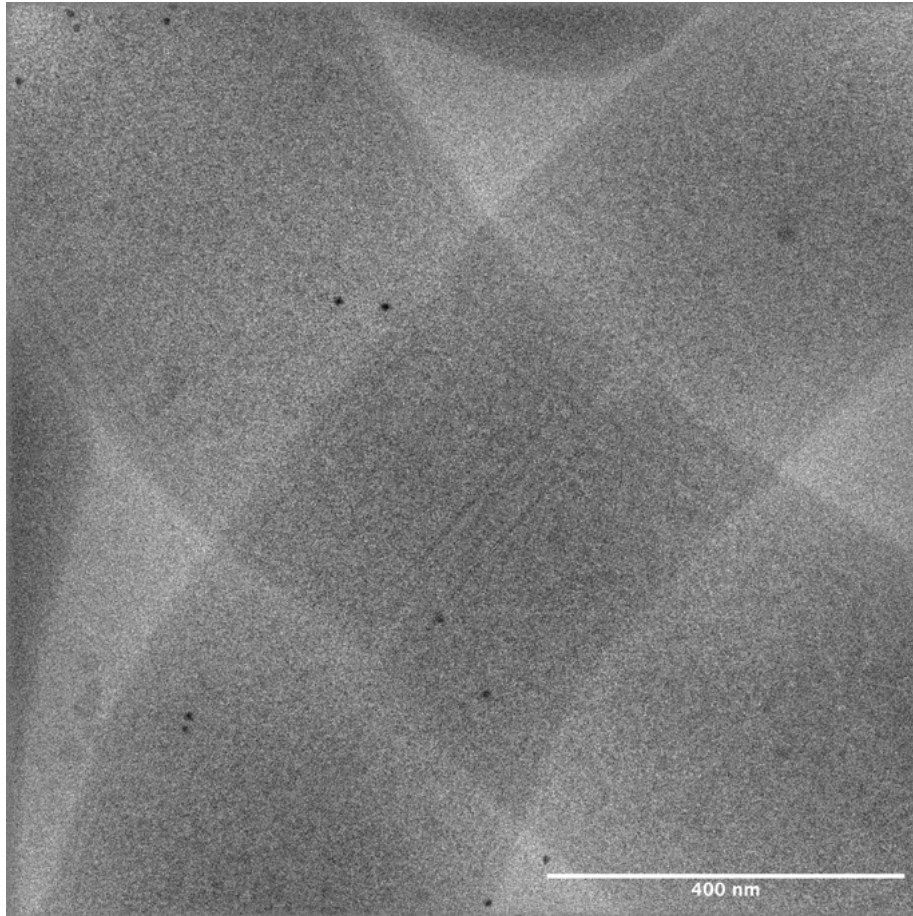


Ptychography Reconstruction (py4Dstem)



Resolution

Max-Leo Leidl, Knut Müller-Caspary



Thick Sample Tomography

- Effects of dynamic scattering can partly be mitigated by **multi-slice ptychography**

====> **Manuel Guizar-Sicairos, PSI & EPFL**

- Larger tilt angle increments are possible due to thicker slabs in Fourier space (Crowther criterion)
- A 3D reconstruction with some modest data in the missing wedge can be computed.

Cryo-electron ptychography image of overlapping microbacteria (Sample thickness >600nm)

See also the work of Sharon Wolf, Michael Elbaum, or Dave Muller (Cornell) et al.

LBEM – Laboratory of Biological Electron Microscopy, Inst. of Physics, EPFL

Titan Krios G4
(2022)

cold-FEG

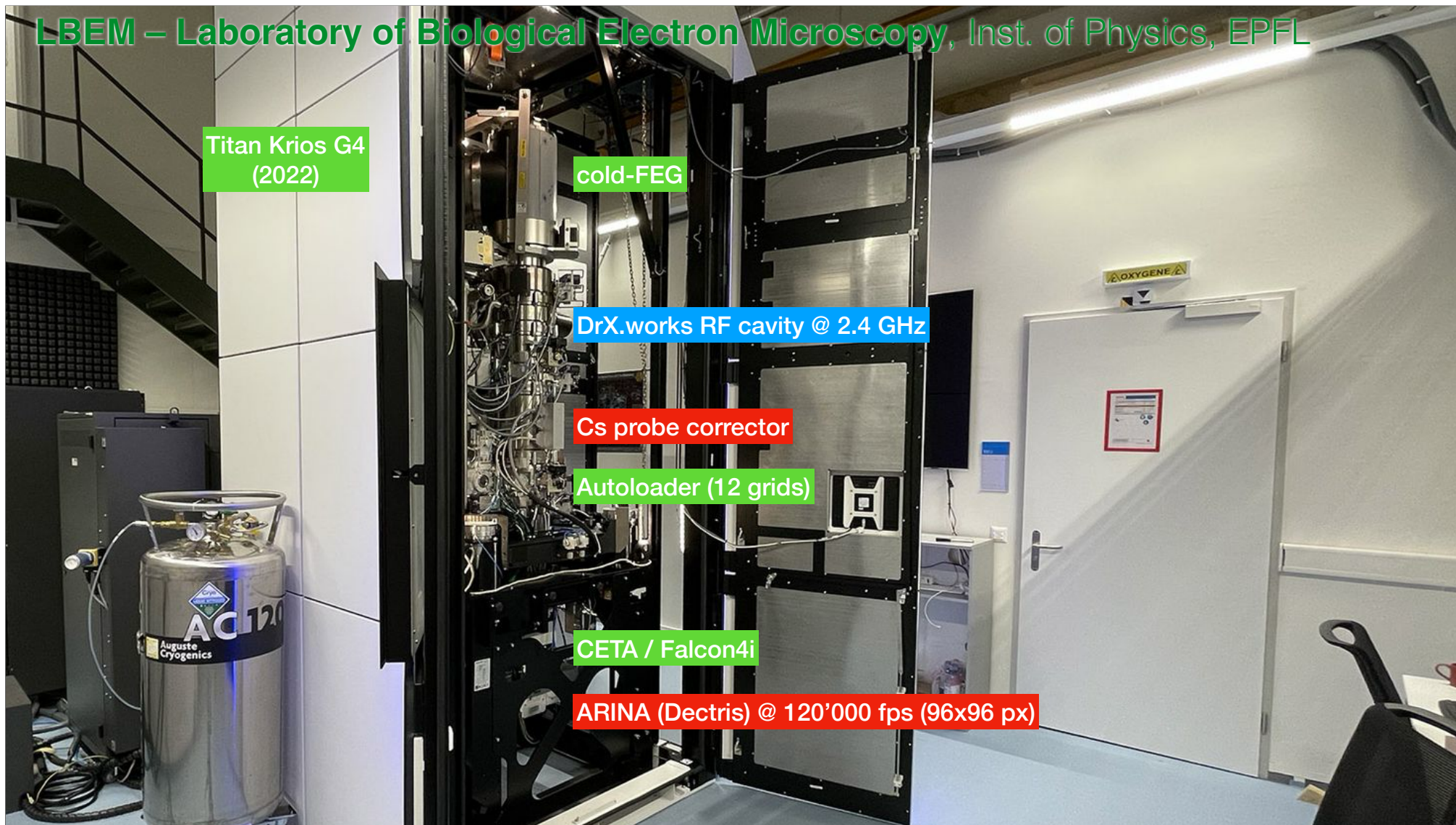
DrX.works RF cavity @ 2.4 GHz

Cs probe corrector

Autoloader (12 grids)

CETA / Falcon4i

ARINA (Dectris) @ 120'000 fps (96x96 px)



Louis de Broglie



Prince Louis-Victor Pierre Raymond de Broglie

Dualism:
Is the electron a wave?
Is the electron a particle?
==> It is both !

PhD Thesis 1924

RADIATIONS. — *Ondes et quanta* (1).
Note de M. **LOUIS DE BROGLIE**.

Considérons un mobile matériel de masse propre m_0 se mouvant par rapport à un observateur fixe avec une vitesse $v = \beta c$ ($\beta < 1$). D'après le principe de l'inertie de l'énergie, il doit posséder une énergie interne égale à $m_0 c^2$. D'autre part, le principe des quanta conduit à attribuer cette énergie interne à un phénomène périodique simple de fréquence ν_0 telle que

$$h \nu_0 = m_0 c^2,$$

c étant toujours la vitesse limite de la théorie de relativité et h la constante de Planck.

Pour l'observateur fixe, à l'énergie totale du mobile correspondra une fréquence $\nu = \frac{m_0 c^2}{h \sqrt{1 - \beta^2}}$. Mais, si cet observateur fixe observe le phénomène périodique interne du mobile, il le verra ralenti et lui attribuera une fréquence $\nu_1 = \nu_0 \sqrt{1 - \beta^2}$; pour lui, ce phénomène varie donc comme

$$\sin 2\pi \nu_1 t.$$

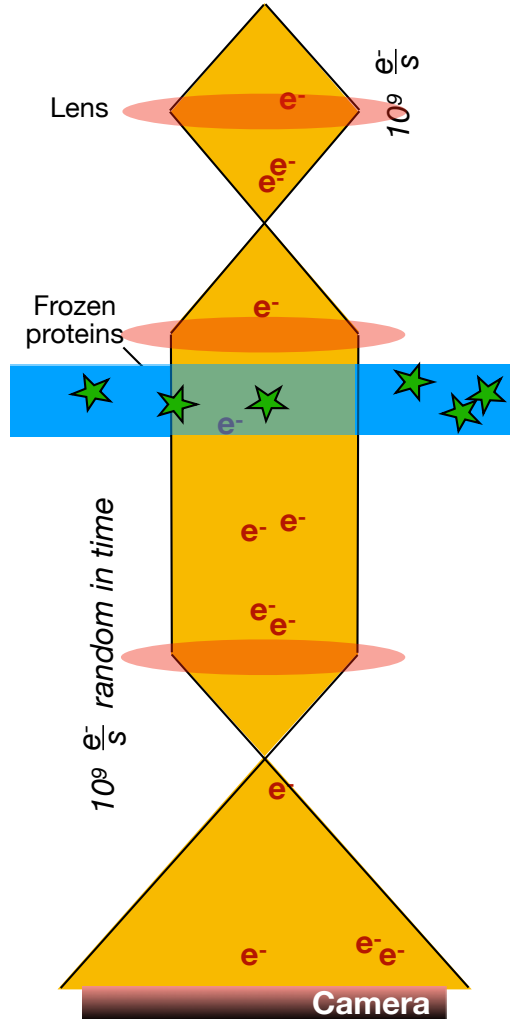
Supposons maintenant qu'au temps $t = 0$, le mobile coïncide dans l'espace avec une onde de fréquence ν ci-dessus définie se propageant dans la même direction que lui avec la vitesse $\frac{c}{\beta}$. Cette onde de vitesse plus grande que c ne peut correspondre à un transport d'énergie; nous la considérerons seulement comme une onde fictive associée au mouvement du mobile.

Je dis que, si au temps $t = 0$, il y a accord de phase entre les vecteurs de l'onde et le phénomène interne du mobile, cet accord de phase subsistera. En effet, au temps t le mobile est à une distance de l'origine égale à $\nu t = x$; son mouvement interne est alors représenté par $\sin 2\pi \nu_1 \frac{x}{v}$.

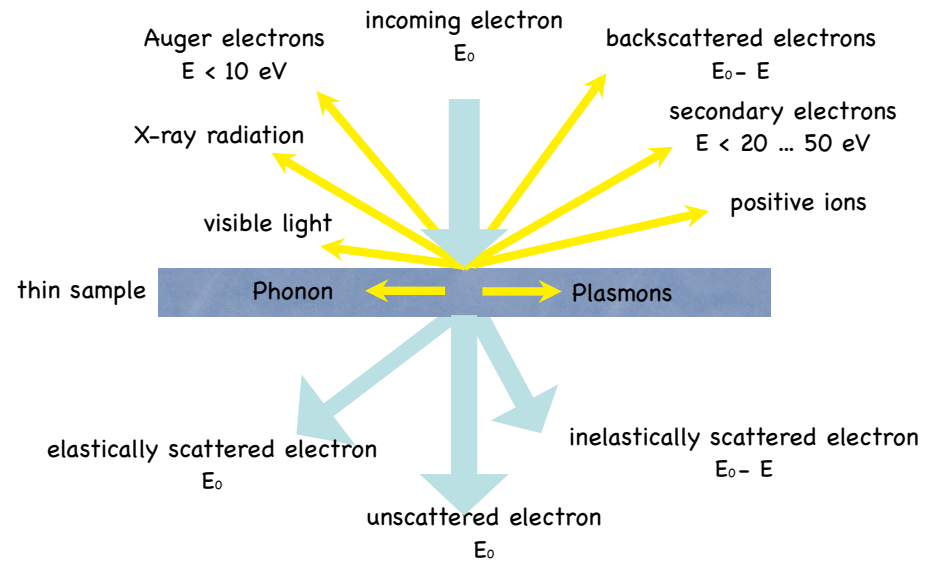
(1) Au sujet de la présente Note, voir M. BRILLOUIN, *Comptes rendus*, t. 168, 1919, p. 1318.

EM: Beam / Sample interaction

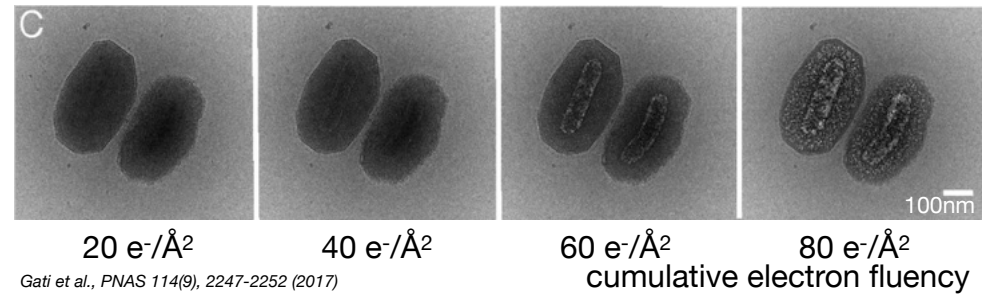
Conventional electron source



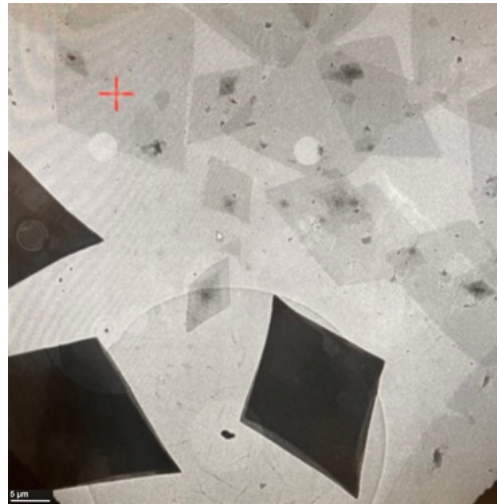
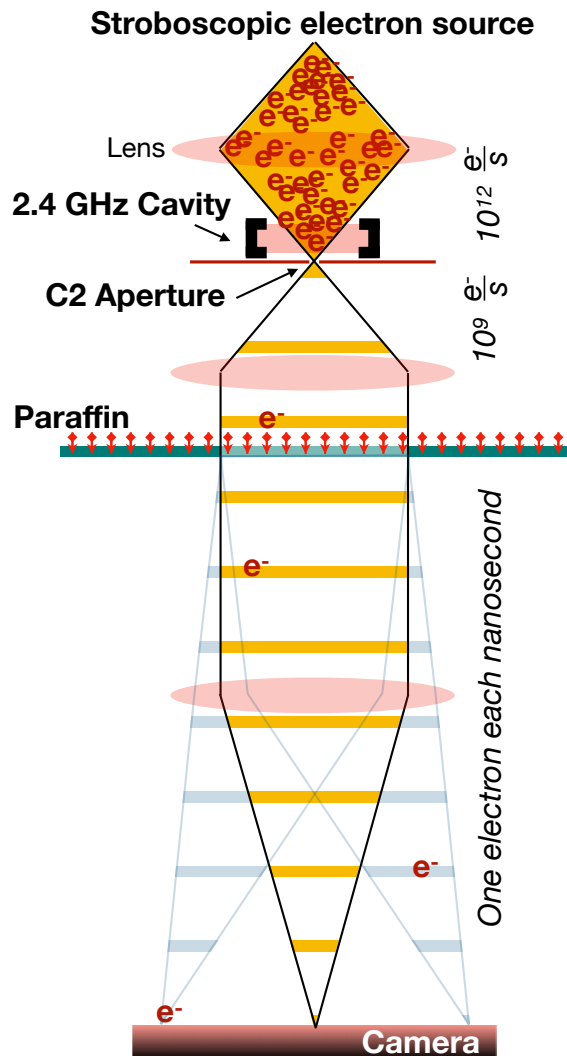
Electron Sample Interaction



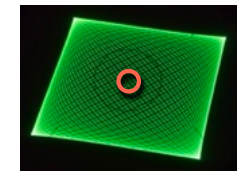
Granulovirus



Paraffin 2D Crystal under stroboscopic single electron diffraction



Tetratetracontane ($\text{C}_{44}\text{H}_{90}$)
Orthorhombic crystal structure

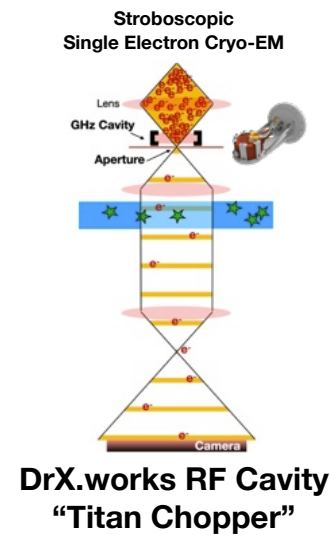


Electron diffraction

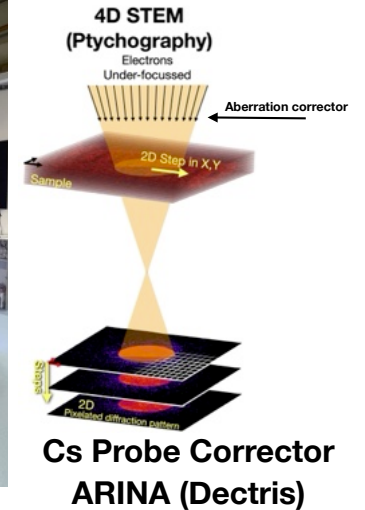
	X/Y Lissajous
Beam Frequency	75 MHz
Beam at gun	60.0 nA (!!!)
Beam on sample	4 pA
Beam diameter	548 nm
Fluency rate at sample	$1.1 \text{ e}^-/\text{A}^2/\text{s}$
Pulse length	0.9 ps / 13.33 ns
On/Off ratio	1 : 15'000
Probability of 1 e- per gate	24.5%
Probability of 2 e- per gate	4.2%
Probability of 3 e- per gate	0.5%

Biology:
Parkinson's
Disease

Physics:
4D-STEM



300kV Cold FEG



ETHZ
Roland Riek
Paola Picotti
Tatiana Serdiuk

Uni Basel
Thomas Braun

CNRS Paris
Ronald Melki
Alexis Fenyi

VUMC, Amsterdam
Wilma van de Berg
Annemieke J.M. Rozemuller;

CNRS Bordeaux
François Ichas
Luc Bousset

EPFL
Hilal Lashuel

MRC, Cambridge
Richard Henderson

TU München
Knut Müller-Caspary
Max-Leo Leidl

ER-C Jülich
Carsten Sachse

Weizmann, Israel
Michael Elbaum
Shahar Seifer

SLS Detector Group, PSI
Bernd Schmitt
Erik Fröjd

TFS, Eindhoven
Erik Kit
Mark Rjit
Ryan Ingenhoest

Hoffmann-La Roche, Basel
Matthias Lauer
Markus Britschgi



Christel Genoud
Alex Myasnikov
Emiko Uchikawa
Sergey Nazarov
Bertrand Beckert
Inay Mohamed
Florent Wenger
Mireille Fasmeyer

EMF, UNIL

Christel Genoud
Jean Daraspe

IPHYS-IT, EPFL

Gaël Cartier-Michaud
Alexandre Guerne

PTPSP, EPFL

Florence Pojer
Kelvin Lau

Domenic Burger
Marta di Fabrizio
Babatunde Ekundayo
Kazadi Ekundayo
Mireille Fasmeyer
Sandor Kasas
Massimo Kube
Berk Küçükoglu
Vishal Kumar
Chinmaya KV
Amanda Lewis
Dongchun Ni
Julika Radecke
Sergey Sekatski
Notash Shafiei
Daniel Stähli
Meltem Tatli
Lukas van den Heuvel
Inés Villalba

